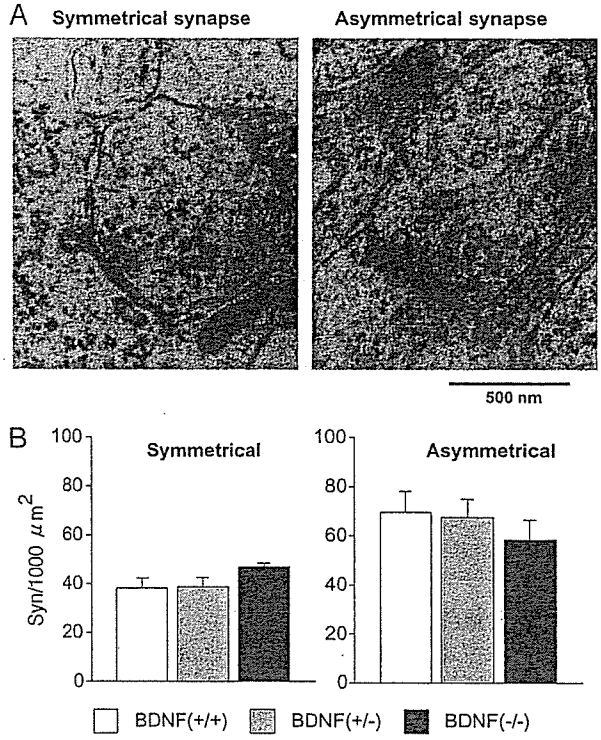

Fig. 1. Synaptic structure in the developing somatosensory cortex in the wild-type mouse at P8. (*A*) (*Left*) Symmetrical synapse. (*Right*) Asymmetrical synapse. (Bar = 500 nm.) (*B*) Comparison of synaptic density (number/1,000 μm^2) of symmetrical and asymmetrical synapses among three genotypes.

dye tracing of thalamocortical projections (10). To see more detailed structural abnormality in the knockout mouse, we carried out electron microscopic analysis of barrel neurons just after the critical period (P8). First we compared the synaptic density among BDNF genotypes. It has been shown that BDNF regulates the central synapse density (14). However, in the barrel cortex, no significant difference of synaptic density was observed, either symmetrical or asymmetrical, among genotypes (Fig. 1). Among asymmetrical synapses, ≈25% are attributed to glutamatergic thalamocortical synapses (13). Next, we measured the synaptic junction length and compared the result among genotypes. Both BDNF(+/−) and BDNF(−/−) showed smaller synaptic contact size compared with wild type (Table 1). In contrast, no significant difference was observed with asymmetrical synapses containing a low number of vesicles in the synapses (Table 1). In hippocampal neurons, the synaptic contact size positively correlated with the number of AMPAR in postsynaptic density (PSD) (15). Thus the shorter synaptic junction length in BDNF knockout mice may suggest less insertion of AMPAR in PSD.

Table 1. Synaptic junction lengths

	Synaptic vesicles (+)	Synaptic vesicles (−)
BDNF(+/+)	373.8 ± 8.4 (256)	290.4 ± 9.1 (146)
BDNF(+/−)	337.3 ± 7.4 (279)*	299.0 ± 8.8 (151)
BDNF(−/−)	343.0 ± 8.1 (228)*	308.5 ± 7.8 (165)

The difference in synaptic junction lengths among BDNF genotypes. The synaptic contact size was estimated as described in *Supporting Methods*. We defined the vesicle containing (+) and not containing (−) synapses according to the number (more than four and less than three, respectively) of synaptic vesicles appeared at the proximal region of postsynaptic density, as shown in Fig. 1*A*. The number in parentheses is the synaptic number examined. The data are shown as average length (nm) ± SEM. Significance was shown by the asterisk when $P < 0.05$ by using the Mann–Whitney *U* test.

Abundance of "Silent" Synapses in BDNF Knockout Mice Even After the Critical Period. Next we examined the normal development of cortical glutamatergic transmission by using acute thalamocortical slices under whole-cell patch recording conditions. At P4, the

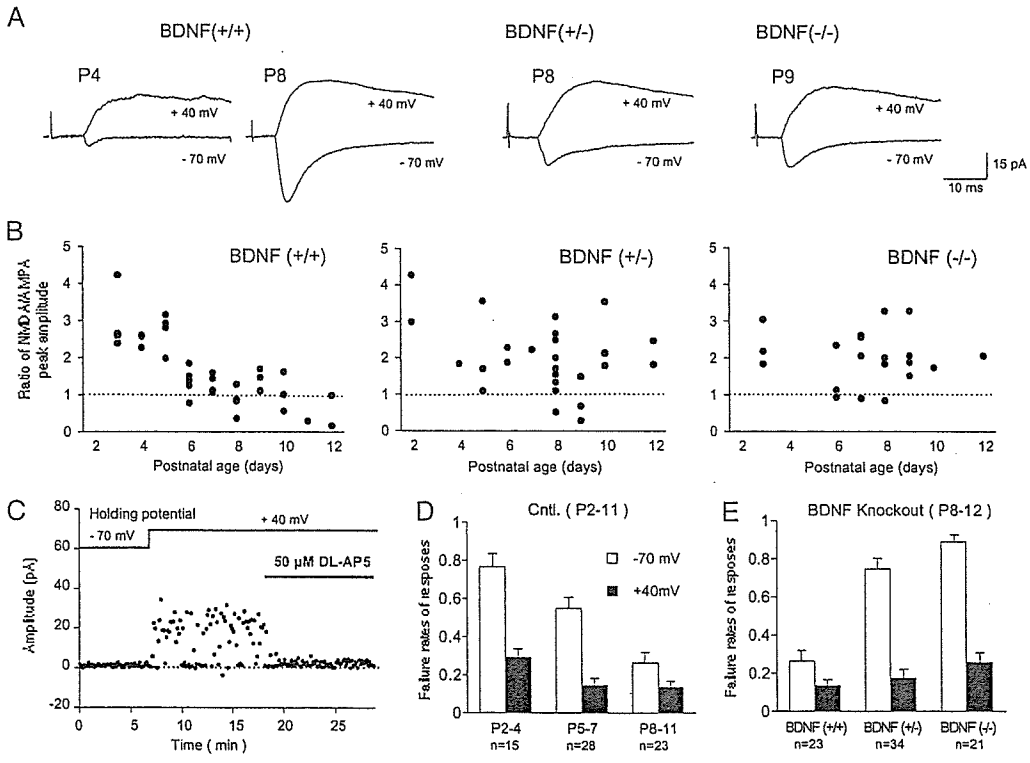

Fig. 2. Higher incidence of silent synapses in BDNF knockout mice compared with wild-type mice during postnatal development. (*A*) Developmental shift of the ratio of NMDAR- to AMPAR-mediated currents in wild-type mice and knockouts. Typical sweeps from P4, P8, or P9 mice are shown. (*B*) The ratio of NMDAR-mediated synaptic peak currents to AMPAR-mediated synaptic peak currents as a function of age among three genotypes. (*C*) An experiment demonstrating the existence of NMDAR-only synapses (P4). (*D*) Decrease in mean failure rates of glutamatergic EPSCs at −70 mV (open bars) and +40 mV (filled bars) holding potentials during postnatal development. Postnatal age (P) and number of experiments (*n*) are indicated below the bars. (*E*) More abundant NMDAR-only synapses in knockouts compared with wild-type mice at P8–P12. Open and filled columns show mean failure rates at −70 mV and 40 mV holding potential, respectively. For raw values, see Table 2.

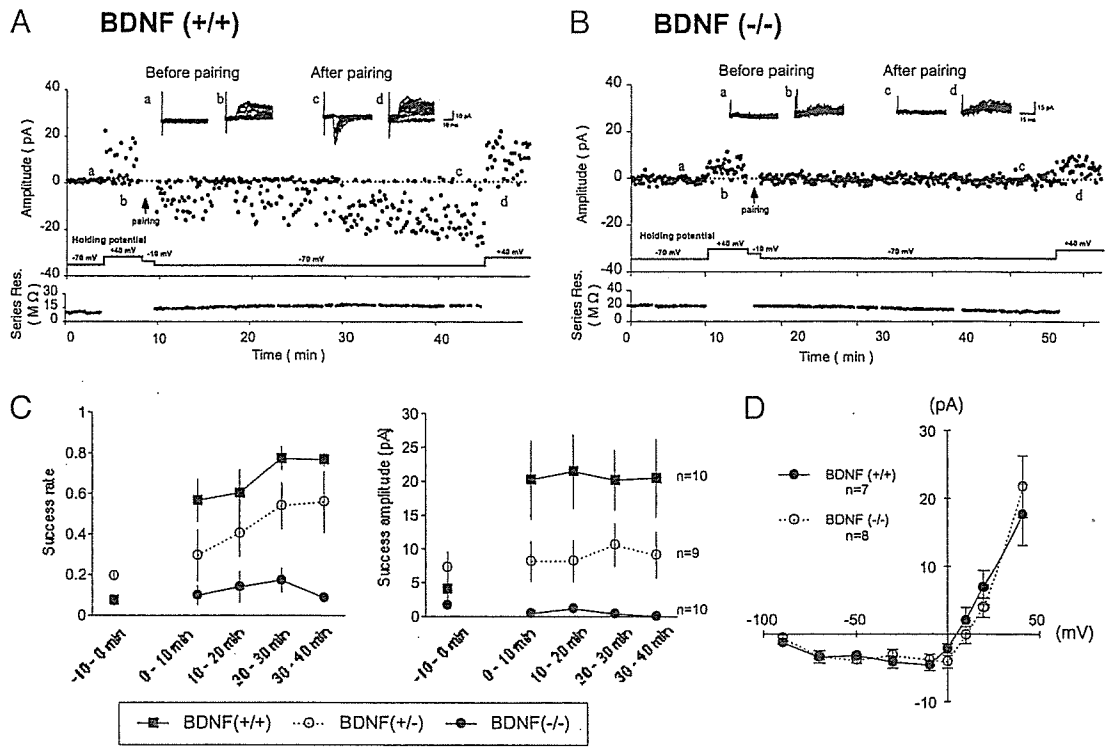

Fig. 3. BDNF requirement for conversion of NMDAR-only synapses. (*A*) A typical example of the conversion of NMDAR-only synapses by pairing stimulation. Black arrow indicates the timing of pairing stimulation. Series resistance (Series Res.) is plotted below. (*Inset*) Overlay of 15 baseline responses before (*a* and *b*) and 30 min after (*c* and *d*) pairing at −70 mV and at +40 mV, respectively. (*B*) The failure of conversion of NMDAR-only synapse in a P8 BDNF(−/−) mouse by pairing stimulation. (*C*) Summary of conversion of NMDAR-only synapses. (*Left*) Mean success rates at −70 mV holding potential before (−10 to 0 min) and after pairing at the specified time window. (*Right*) Mean success amplitude at −70 mV holding potential before and after pairing. For more detailed raw data, see Tables 2 (success rates) and 3 (success amplitudes). (*D*) Normal ratio of NMDAR-mediated currents to AMPAR-mediated currents in the BDNF(−/−) compared with the wild-type mouse.

NMDAR current was prominent, whereas the AMPAR current was minor (Fig. 2*A Left*). At P8, both NMDAR and AMPAR currents were observed. Thus, the relative contribution of NMDAR vs. AMPAR currents decreased during P2–P12 (Fig. 2*B Left*). In contrast, the relative NMDAR currents are still prominent in both BDNF(+/−) and BDNF(−/−) mice even at P8 (Fig. 2*A Center* and *Right*, and Fig. 2*B Center* and *Right*). To see whether this high ratio relates to the silent synapse, we measured the failure rate at minimum stimulation in which synaptic transmission shows failure (for more details, see *Supporting Methods*). A typical example of NMDAR-only transmission from P4 mice is shown in Fig. 2*C*. Synaptic transmission was not observed at −70 mV at all but was detected at +40 mV, which is sensitive to the NMDAR antagonist, AP5. Statistically, the failure rate of AMPAR was high (0.77 ± 0.07, $n = 15$) in P2–P4 and rapidly lowered below 0.26 and P8–P11 (Fig. 2*D*). However, the failure rate of NMDAR was low (0.29 ± 0.05, $n = 15$) even at P2–P4 and decreased below 0.13 at P8–P11 (Fig. 2*D*). This result suggests that NMDAR-only synapses are prominent at the beginning of the critical period (P2–P6), confirming previous observations by other researchers (16). However, the failure rate of AMPAR compared with that of NMDAR is selectively high even after P8 in BDNF knockout mice (Fig. 2*E*). These data suggest that silent synapses are prominent and not converted into active ones in the BDNF knockout mouse.

Impaired Unmasking of "Silent" Synapse in BDNF Knockout Mice. The activation of NMDAR current-only synapses into AMPAR current-containing ones could be induced by a pairing stimulation, as described in *Supporting Methods* (Fig. 3*A*). The failure rate of AMPAR was gradually decreased over 20 min after the pairing stimulation (see also summary data in Fig. 3*C*). The reason for this gradual increment is uncertain. Note that the failure rate as well as the success amplitude of NMDAR did not change before and after pairing stimulation (Fig. 4*C* and Table 2, which is published as supporting information on the PNAS web site). This result indicates that pairing stimulation selectively improved AMPAR transmission in NMDAR-only synapses. The same pairing stimulation, however, could not induce activation of silent synapses in the BDNF(−/−) mouse (Fig. 3*B*). The time courses of improvement of the success rate (one-failure rate) as well as success amplitude were summarized (Fig. 3*C*). In BDNF(+/−), a little improvement in success rate (Fig. 3*C* and Table 2), but not of success amplitude, was statistically significant (Fig. 3*C* and Table 3, which is published as supporting information on the PNAS web site). AP5 blocked the activation of silent synapses in wild-type slices (data not shown), suggesting that NMDAR function is essential for conversion. However, we did not find any difference in current–voltage plot of NMDAR between BDNF(+/+) and BDNF(−/−) mice (Fig. 3*D*). Therefore, the deficit of the activation of NMDAR-only synapses into AMPAR-containing ones should be caused by a signaling mechanism other than NMDAR transmission itself.

Rescue of the Impaired Unmasking of "Silent" Synapses by Exogenous BDNF. If BDNF had a direct role in the conversion of NMDAR current-only synapses into AMPAR current-containing ones, we could expect that the defect should be reversible on adding BDNF back to the acute slices from the knockout mice, which was the case. The acute slices had been preincubated with BDNF for at least 60 min, then BDNF was further included during recording. Thus applied BDNF (20 ng/ml) partially activated NMDAR-only synapses without pairing stimulation (Fig. 4 *A* and *C*). Meanwhile, pairing stimulation fully activated the silent synapses (Fig. 4 *B* and

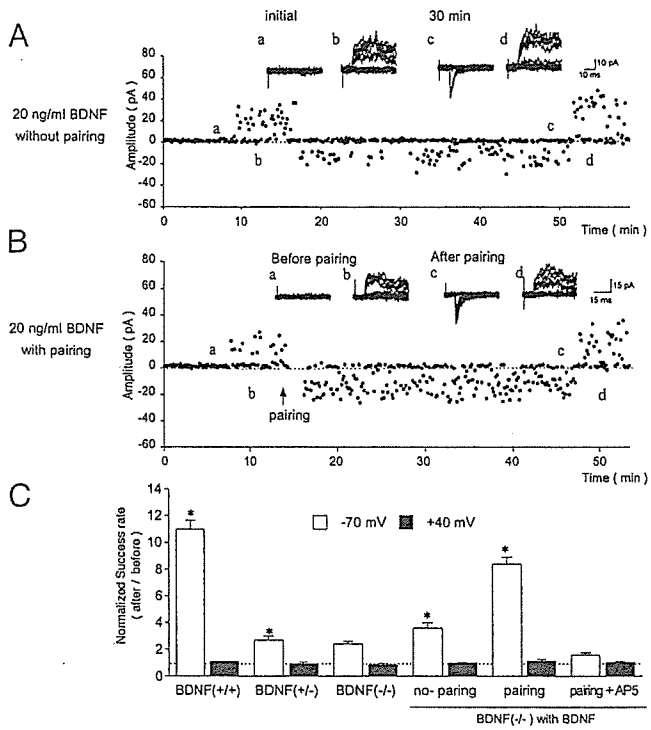

Fig. 4. Rescue of BDNF knockout mouse phenotype by exogenously added BDNF. (*A*) Time course of NMDAR-only synapses recording in the BDNF(−/−) mouse in the presence of exogenous BDNF without pairing stimulation. Slices were preincubated in solution containing 20 ng/ml BDNF before (for at least 1 h) and during experiments. (*Inset*) Overlay of 15 baseline responses, initial (*a*), at −70 mV and 30 min after returning to −70 mV (*c*), and at +40 mV (*b* and *d*), are presented. (*B*) Time course of conversion of NMDAR-only synapses in the BDNF(−/−) mouse with pairing stimulation in the presence of BDNF as described above. (*C*) A summary of rescue experiments showing the normalized success rate at −70 mV. The success rate at +40 mV did not change by pairing stimulation and is normalized as assuming the success rate before pairing to be 1. Only changes in the success rate at 20–30 min after pairing stimulation are presented. Raw values are presented in Tables 2 (success rates) and 3 (success amplitude).

C) and was blocked by AP5 (Fig. 4*C*), indicating that NMDAR-mediated Ca^{2+} transient is required for the BDNF effect. During the rescue experiment, NMDAR transmission did not change in terms of success rate (Fig. 4*C* and Table 2) as well as success amplitude (Table 3), suggesting that the effect of BDNF is selective on the AMPAR transmission at the postsynaptic site. It was reported that BDNF activated NMDAR through shifting the channel into the open state in the hippocampal culture (17). The critical step regulated by BDNF may be different depending on experimental conditions. A 20-min bath application of BDNF during recording was not effective, presumably because of the reluctant penetration of BDNF inside the slice (18). In our case, it needs at least a 60-min preincubation before recording (19).

AMPAR Trafficking as an Essential Step for Unmasking. AMPAR trafficking is supposed to be the molecular basis for the activation of silent synapses in hippocampus neurons (20, 21). To examine a similar possibility in the developing thalamocortical synapse, we postsynaptically applied C-terminal peptides of AMPAR subunits. The C-terminal residues of a long form of GluR1 form a group I PDZ ligand and are essential for interaction with the PDZ-domain regions of SAP97. The nine-residue peptide (GMPLGATGL) of a GluR1 C-terminal tail selectively blocked the activation of NMDAR-only synapses on pairing stimulation without affecting NMDAR transmission (Fig. 5 *A*, *E*, and *F*). In contrast, a mutated peptide (GMPLGAAGL) losing interaction with SAP97 did not block the conversion (Fig. 5 *B*, *E*, and *F*). Similarly, the 10-residue peptide (NVYGIESVKI) of a GluR2 C-terminal tail forms a group II PDZ ligand and is essential for interaction with ABP/GRIP. This peptide blocked conversion when applied postsynaptically (Fig. 5 *C*, *E*, and *F*). The conversion, however, was not blocked by a mutated peptide (NVYGIEAVKI) (Fig. 5 *D–F*), which lost ABP/GRIP binding but still binds with PICK1 (22). This result suggests that the interaction of GluR2R with ABP/GRIP is more important than that of GluR2 with PICK1 to recruit or stabilize the receptor in the synaptic site. The success amplitude of AMPAR was not affected by the mutated peptides (for raw values, see Table 3). The time course of the success amplitude with these peptides is also provided as Fig. 7, which is published as supporting information on the PNAS web site. Taken together, these results suggest that AMPAR subunit recruiting or stabilization into synaptic sites underlies a molecular mechanism for the conversion of NMDAR-only synapses into active ones. To examine any abnormal expression of glutamate receptors and their interacting proteins in knockout mice, we performed Western blotting analysis with a cell extract preparation of P8 barrel cortex using the following antibodies: NR1, NR2A, NR2B, NR2C, GluR1, GluR2/3, NSF, α-actinin, PSD95, SAP102, GRIP, and PICK1. We found no significant deficit (data not shown), consistent with the notion that delivery and/or interaction may be impaired in the absence of proper doses of BDNF.

Critical Role of Postsynaptic TrkB and Ca^{2+} Rise. Next we investigated a possible molecular mechanism of BDNF to regulate AMPAR trafficking into the synaptic site. First, we examined the site of BDNF action by postsynaptically applied K252b, a membrane-impermeable Trk tyrosine kinase inhibitor (ref. 23, but see also ref. 24). At 13 ng/ml, 29 nM, this inhibitor blocked the conversion of NMDAR-only synapses into AMPAR-transmissible ones without affecting NMDAR transmission (Fig. 6*A*). This result suggests that BDNF affects AMPAR trafficking through its postsynaptic receptor. BDNF elicited the postsynaptic Ca^{2+} transients (5, 25), leading to the induction of long-term potentiation (LTP). Thus, we examined a membrane-impermeable Ca^{2+}-chelating agent, 1,2-bis(2-aminophenoxy)ethane-*N,N,N′,N′*-tetraacetate or -tetraacetic acid (BAPTA). BAPTA postsynaptically blocked activation of the silent synapse, suggesting that postsynaptic transient Ca^{2+} is important for AMPAR trafficking. Next, we examined the role of PLC-γ, because among the possible downstream targets of the TrkB receptor, PLC-γ is reported to be essential for induction of LTP (26–28). A selective inhibitor of PLC-γ, U73122, but not the inactive counterpart, U73343, blocked activation (Fig. 6*B*). These results are consistent with the importance of Ca^{2+} transients for AMPAR trafficking. All experiments described above were carried out in the presence of a γ-aminobutyric acid (GABA) type A receptor ($GABA_A$ R) antagonist, bicuculline; thus, we could exclude the possible involvement of polysynaptic inhibition.

Discussion

In this study, we have presented evidence that endogenous BDNF is essential for unmasking "silent" synapses in the developing mouse barrel cortex. BDNF has been shown to regulate multiple steps to form a functional synapse. First, BDNF exerts morphological effect on both axons and dendrites, enhancing the surface area of these structures, thus increasing the number of potential contact sites (permissive effect) (12, 29). Second, BDNF more directly regulates synaptic efficacy through pre- and/or postsynaptic mechanisms (instructive effect) (12, 14, 30, 31). An intensive morphological study of hippocampal synaptogenesis in *trk*B(−/−) and *trk*C(−/−) mice revealed that the topographic patterns of hippocampal connections are normal, but the morphology of axons and dendrites as well as pre- and postsynaptic structures are reduced (14). In the developing barrel cortex, synaptic density is normal, but synaptic contact size is reduced in both BDNF(+/−) and BDNF(−/−) just

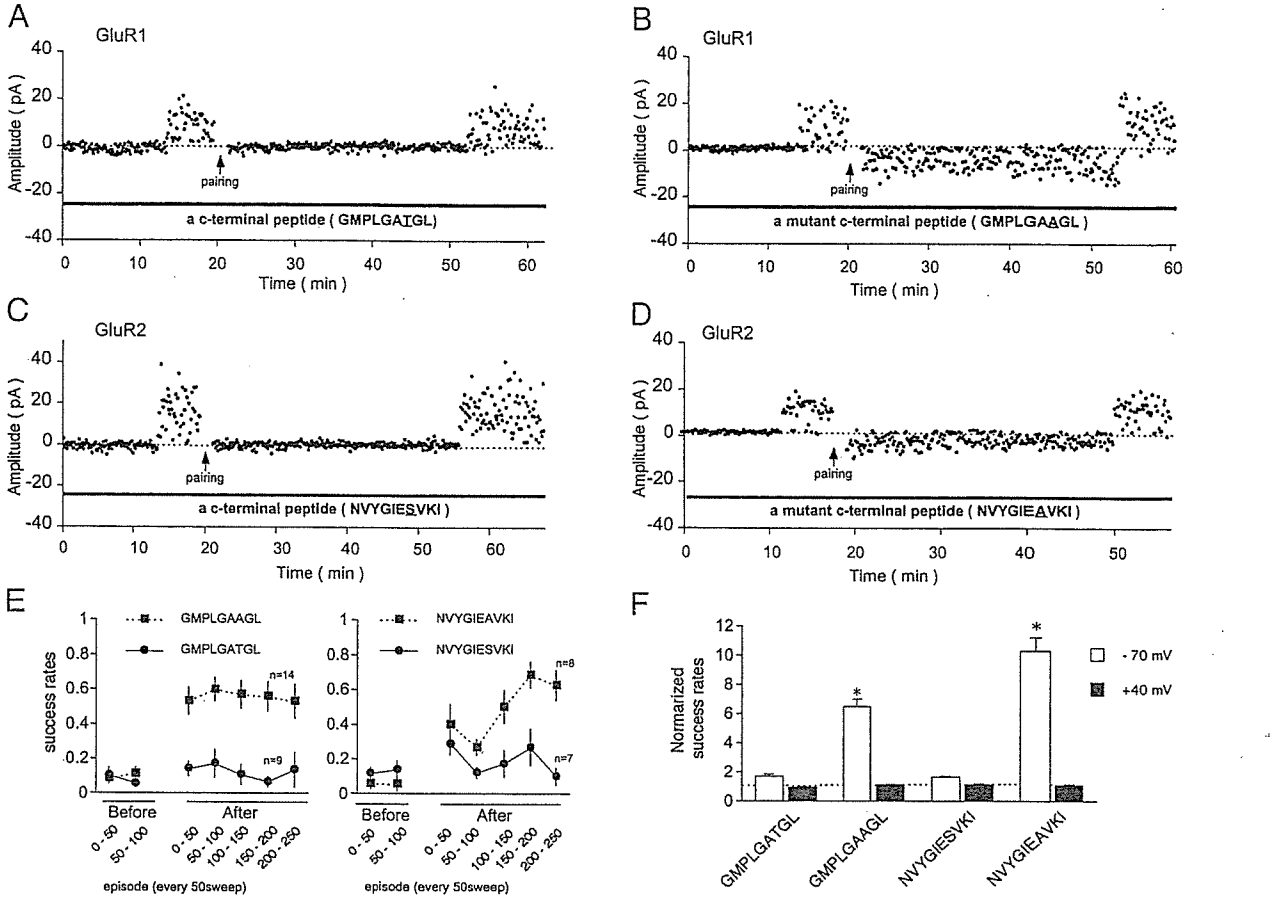

Fig. 5. The blocking of AMPAR transmission by postsynaptically applied C-terminal peptides of GluR1 and -R2 receptors. (*A* and *B*) An effect of a SAP97-binding GluR1 peptide. (*A*) A normal peptide (GMPLGATGL). (*B*) A mutated peptide (GMPLGA*A*GL) losing SAP97 binding activity. (*C* and *D*) Effect of a GRIP-binding GluR2 peptide. (*C*) A normal peptide (NVYGIESVKI). (*D*) A mutated peptide (NVYGIE*A*VKI) losing ABP/GRIP-binding activity. (*E*) Time course of changes in success rates at −70 mV after pairing in the presence of the C-terminal peptides of GluR1 (*Left*) and -R2 (*Right*). (*F*) Normalized success rates of steady-state synaptic AMPAR- (open bar) and NMDAR-mediated responses (filled bar) in neurons injected with the GluR1/GluR2 C-terminal peptides. Normalized success rates show changes in the success rate 20–30 min after pairing stimulation (see Table 2 for success rates, and see Table 3 and Fig. 7 for success amplitudes).

after the critical period (P8). Membrane properties of barrel neurons seemed normal among BDNF genotypes (data not shown). These results suggest that the unmasking of silent synapses by BDNF is instructive rather than permissive, which remains to be further clarified.

We found that activity and BDNF work synergistically to convert NMDAR-only synapses into AMPAR-containing ones. Neuronal activity is thought to locally secrete neurotrophins, which modulate pre- and/or postsynaptic efficacy (32–34). In our analysis, BDNF alone significantly, but not completely, rescued the defect of unmasking silent synapses in BDNF knockout mice in the absence of pairing electric stimulation. Thus, we propose that neuronal activity is required also for a mechanism other than BDNF secretion. Neuronal activity may be required for activation of NMDAR by coincident activation of pre- and postsynaptic sites. If this is so, we wonder why BDNF is required further in the conversion of silent synapses, because BDNF itself induces postsynaptic Ca^{2+} rise (5, 25). A prevailing idea is that the summation of Ca^{2+} concentration above the threshold level is essential for the induction of long-term potentiation (35). However, it should be clarified whether this is the case in the activation of silent synapses. Not only absolute concentration but also a speciotemporal pattern of intracellular Ca^{2+} transients may also be important (36, 37). Alternatively or together with NMDAR activation, neuronal activity may enhance the BDNF effect through other glutamate receptors. Metabotropic glutamate receptor is a candidate, because its function and downstream PLC-β1 are essential for cortical barrel development (38). The kainate receptor, having a relatively long-lasting depolarization, was found in developing thalamocortical synapses, and its activity was developmentally reduced during the critical period (39). Furthermore, the monoamine oxidase mutant (40) as well as the type I adenylate cyclase mutant mouse (41) showed a barrelless phenotype, and interactions between TrkB signaling and serotonin were suggested (42). Considering these findings, we speculate that modulators, including monoamine, catecholamine, and acetylcholine, are gating factors for BDNF potentiation in developing NMDAR-only synapses. In neuromuscular junctions, BDNF and activity synergistically potentiated presynaptic release (43) and the activity-dependent translocation of TrkB may be a molecular basis of this synergism (44). For insight into the possible contribution of presynaptic transmission in our system, we recorded miniature excitatory postsynaptic currents (EPSCs) just after pairing stimulation and compared the result between BDNF(+/+) and BDNF(−/−). Both mEPSC frequency and amplitude at −70 mV did not differ between BDNF(+/+) (n = 7) and BDNF(−/−) (n = 4) (0.13 ± 0.04 and 0.18 ± 0.07 Hz, and 18.4 ± 3.04 and 17.1 ± 4.34 pA, respectively) (For more detailed information, see Fig. 8, which is published as supporting information on the PNAS web site). However, we cannot at this moment exclude the possibility of improvement of presynaptic transmission during or after the conversion of silent synapses. BDNF alone significantly activates silent synapses (Fig. 4*A*). What might the mechanism be? BDNF could

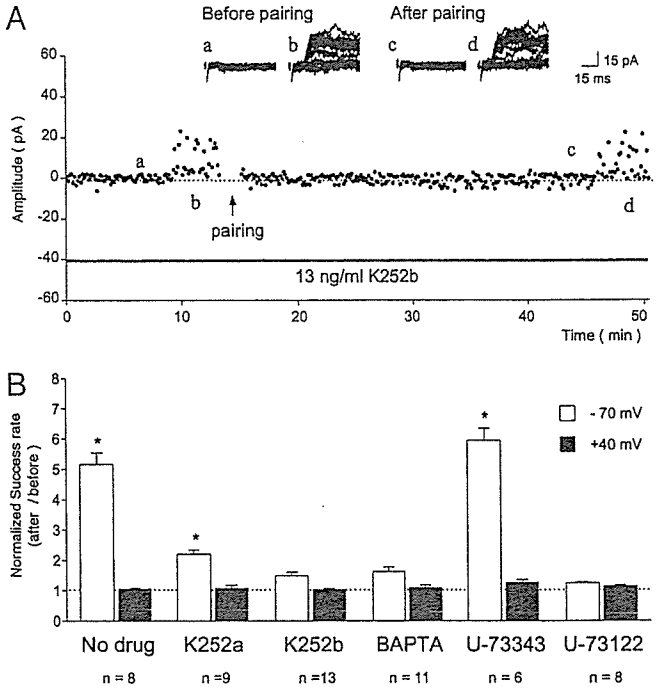

Fig. 6. Postsynaptic TrkB receptor kinase activity and calcium signaling-dependent conversion of NMDAR-only synapses. (*A*) K252b blocked the conversion of NMDAR-only synapses in the P5 wild-type mouse. Responses within a few minutes after forming the whole-cell configuration and after 10 min of loading K252b did not change. (*B*) Summary of the effect of various drugs on the conversion of NMDAR-only synapses in wild-type mice (P3–P6). The relative increment of the success rate is shown as assuming the success rate before pairing to be 1. Success rates were obtained 20–30 min after pairing. Raw values are presented in Tables 2 (success rates) and 3 (success amplitudes).

activate the Na(V)1.9 channel through TrkB kinase activity (45). Another possibility is the induction of Ca^{2+} influx through the activation of a nonselective cation channel (TRPC3) (46), which is an internal store-operated channel. TRPC3 protein is enriched in the central nervous system during embryonic day 18 and P20 in rat brain and colocalized with TrkB.

A molecular mechanism of AMPAR trafficking is now under intensive study in many laboratories, because the regulation of AMPAR-exocytotic and -endocytotic sorting (recycling) is a critical mechanism of synaptic potentiation (9, 12). Many molecules belonging to different functional categories have been studied, including PSD95, Stargazin, NSF-ATPase, ABP/GRIP, PICK1, and ubiquitin-dependent regulators. It is too early, however, to unify the regulatory mechanism of AMPAR recycling. It is of note that a rate-limiting step of AMPAR recycling may be different in depending on a neural subtype and a maturational stage of synapses. Spontaneous activity could drive GluR4-containing AMPAR into silent synapses in cultured hippocampal slices (47), and GluR2/3 replaces GluR4/1 in an activity-independent manner (47). In our case, both GluR1 and -R2 seem to be sorted into synaptic sites in an activity-dependent manner (Fig. 5), although the possibility of nonspecific blocking of PDZ-interacting factors by peptides is not excluded in our experiment (47). The development of excitatory synapses is differently regulated by BDNF in depending on the postsynaptic cell type (12, 48). Excitatory synapses on pyramidal neurons are negatively regulated, whereas inhibitory interneurons are positively regulated by BDNF in cortical cultures (30). In hippocampal cultures, BDNF strengthens excitation primarily by augmenting the amplitude of AMPAR-mediated miniature EPSCs but enhances inhibition by increasing the frequency of miniature inhibitory postsynaptic currents and increasing the size of γ-aminobutyratergic synaptic terminals (31). We found the dose-dependent effect of the BDNF gene in the unmasking efficiency of silent synapses (Fig. 3*C*), which may be related to the difference of the BDNF requirement among postsynaptic neuron subtypes. This point remains to be clarified further.

We thank Dr. Yoshinori Sahara for critical reading of the manuscript. This research was supported by an Advanced Brain Research grant from the Ministry of Education, Science, Sport, Culture, and Technology, by Core Research for Evolutional Science and Technology (Japan), by Health Sciences Research Grants (HSRG) from the Organization of Pharmaceutical Safety and Research (MF-3) and Research on Advanced Medical Technology (nano-001).

1. Levi-Montalcini, R., Skaper, S. D., Dal Toso, R., Petrelli, L. & Leon, A. (1996) *Trends Neurosci.* **19**, 514–520.
2. Cline, H. T. (2001) *Curr. Opin. Neurobiol.* **11**, 118–126.
3. Katz, L. C. & Shatz, C. J. (1996) *Science* **274**, 1133–1138.
4. Thoenen, H. (1995) *Science* **270**, 593–598.
5. Kovalchuk, Y., Hanse, E., Kafitz, K. W. & Konnerth, A. (2002) *Science* **295**, 1729–1734.
6. Isaac, J. T., Nicoll, R. A. & Malenka, R. C. (1995) *Neuron* **15**, 427–434.
7. Liao, D., Hessler, N. A. & Malinow, R. (1995) *Nature* **375**, 400–404.
8. Montgomery, J. M., Pavlidis, P. & Madison, D. V. (2001) *Neuron* **29**, 691–701.
9. Malinow, R. & Malenka, R. C. (2002) *Annu. Rev. Neurosci.* **25**, 103–126.
10. Itami, C., Mizuno, K., Kohno, T. & Nakamura, S. (2000) *Brain Res.* **857**, 141–150.
11. Itami, C., Samejima, K. & Nakamura, S. (2001) *Brain Res. Brain Res. Protoc.* **7**, 103–114.
12. Vicario-Abejon, C., Owens, D., McKay, R. & Segal, M. (2002) *Nat. Rev. Neurosci.* **3**, 965–974.
13. White, E. L., Weinfeld, L. & Lev, D. L. (1997) *Somatosens. Mot. Res.* **14**, 34–55.
14. Martinez, A., Alcantara, S., Borrell, V., Del Rio, J. A., Blasi, J., Otal, R., Campos, N., Boronat, A., Barbacid, M., Silos-Santiago, I. & Soriano, E. (1998) *J. Neurosci.* **18**, 7336–7350.
15. Takumi, Y., Ramirez-Leon, V., Laake, P., Rinvik, E. & Ottersen, O. P. (1999) *Nat. Neurosci.* **2**, 618–624.
16. Isaac, J. T., Crair, M. C., Nicoll, R. A. & Malenka, R. C. (1997) *Neuron* **18**, 269–280.
17. Levine, E. S., Crozier, R. A., Black, I. B. & Plummer, M. R. (1998) *Proc. Natl. Acad. Sci. USA* **95**, 10235–10239.
18. Patterson, S. L., Abel, T., Deuel, T. A., Martin, K. C., Rose, J. C. & Kandel, E. R. (1996) *Neuron* **16**, 1137–1145.
19. Akaneya, Y., Tsumoto, T., Kinoshita, S. & Hatanaka, H. (1997) *J. Neurosci.* **17**, 6707–6716.
20. Petralia, R. S., Esteban, J. A., Wang, Y. X., Partridge, J. G., Zhao, H. M., Wenthold, R. J. & Malinow, R. (1999) *Nat. Neurosci.* **2**, 31–36.
21. Zhu, J. J., Esteban, J. A., Hayashi, Y. & Malinow, R. (2000) *Nat. Neurosci.* **3**, 1098–1106.
22. Osten, P., Khatri, L., Perez, J. L., Kohr, G., Giese, G., Daly, C., Schulz, T. W., Wensky, A., Lee, L. M. & Ziff, E. B. (2000) *Neuron* **27**, 313–325.
23. Kinoshita, S., Yasuda, H., Taniguchi, N., Katoh-Semba, R., Hatanaka, H. & Tsumoto, T. (1999) *J. Neurosci.* **19**, 2122–2130.
24. Ross, A. H., McKinnon, C. A., Daou, M. C., Ratliff, K. & Wolf, D. E. (1995) *J. Neurochem.* **65**, 2748–2756.
25. Numakawa, T., Yokomaku, D., Kiyosue, K., Adachi, N., Matsumoto, T., Numakawa, Y., Taguchi, T., Hatanaka, H. & Yamada, M. (2002) *J. Biol. Chem.* **277**, 28861–28869.
26. Atwal, J. K., Massie, B., Miller, F. D. & Kaplan, D. R. (2000) *Neuron* **27**, 265–277.
27. Polleux, F., Whitford, K. L., Dijkhuizen, P. A., Vitalis, T. & Ghosh, A. (2002) *Development (Cambridge, UK)* **129**, 3147–3160.
28. Minichiello, L., Calella, A. M., Medina, D. L., Bonhoeffer, T., Klein, R. & Korte, M. (2002) *Neuron* **36**, 121–137.
29. Wong, R. O. & Ghosh, A. (2002) *Nat. Rev. Neurosci.* **3**, 803–812.
30. Rutherford, L. C., Nelson, S. B. & Turrigiano, G. G. (1998) *Neuron* **21**, 521–530.
31. McLean Bolton, M., Pittman, A. J. & Lo, D. C. (2000) *J. Neurosci.* **20**, 3221–3232.
32. Kohara, K., Kitamura, A., Morishima, M. & Tsumoto, T. (2001) *Science* **291**, 2419–2423.
33. Poo, M-M. (2001) *Nat. Rev. Neurosci.* **2**, 24–32.
34. Patterson, S. L., Pittenger, C., Morozov, A., Martin, K. C., Scanlin, H., Drake, C. & Kandel, E. R. (2001) *Neuron* **32**, 123–140.
35. Bienenstock, E. L., Cooper, L. N. & Munro, P. W. (1982) *J. Neurosci.* **2**, 32–48.
36. Koester, H. J. & Sakmann, B. (1998) *Proc. Natl. Acad. Sci. USA* **95**, 9596–9601.
37. Zhang, L. I. & Poo, M.-M. (2001) *Nat. Neurosci.* **4**, 1207–1214.
38. Hannan, A. J., Blakemore, C., Katsnelson, A., Vitalis, T., Huber, K. M., Bear, M., Roder, J., Kim, D., Shin, H. S. & Kind, P. C. (2001) *Nat. Neurosci.* **4**, 282–288.
39. Kidd, F. L. & Isaac, J. T. (1999) *Nature* **400**, 569–573.
40. Cases, O., Vitalis, T., Seif, I., De Maeyer, E., Sotelo, C., Gaspar, P. & Poo, M-M. (1996) *Neuron* **16**, 297–307.
41. Abdel-Majid, R. M., Leong, W. L., Schalkwyk, L. C., Smallman, D. S., Wong, S. T., Storm, D. R., Fine, A., Dobson, M. J., Guernsey, D. L. & Neumann, P. E. (1998) *Nat. Genet.* **19**, 289–291.
42. Lyons, W. E., Mamounas, L. A., Ricaurte, G. A., Coppola, V., Reid, S. W., Bora, S. H., Wihler, C., Koliatsos, V. E. & Tessarollo, L. (1999) *Proc. Natl. Acad. Sci. USA* **96**, 15239–15244.
43. Boulanger, L. & Poo, M-M. (1999) *Nat. Neurosci.* **2**, 346–351.
44. Meyer-Franke, A., Wilkinson, G. A., Kruttgen, A., Hu, M., Munro, E., Hanson, M. G., Jr., Reichardt, L. F. & Barres, B. A. (1998) *Neuron* **21**, 681–693.
45. Blum, R., Kafitz, K. W. & Konnerth, A. (2002) *Nature* **419**, 687–693.
46. Li, H. S., Xu, X. Z. & Montell, C. (1999) *Neuron* **24**, 261–273.
47. Shi, S., Hayashi, Y., Esteban, J. A. & Malinow, R. (2001) *Cell* **105**, 331–343.
48. Ben-Ari, Y. (2002) *Nat. Rev. Neurosci.* **3**, 728–739.

厚生労働科学研究費補助金

萌芽的先端医療技術推進研究事業

ナノレベルイメージングによる分子の機能および構造解析に関する研究（H14-ナノ-001）

平成14-18年度　総合研究報告書

Vol.4

主任研究者　盛　英三

平成19年（2007年）3月

— Minireview —

Therapeutic Approaches in Prion Disease

Naomi S. Hachiya,[a, b] Yuji Sakasegawa,[a, b] and Kiyotoshi Kaneko*[, a, b]

[a]Department of Cortical Function Disorders, National Institute of Neuroscience, National Center of Neurology and Psychiatry, 4–1–1 Ogawahigashi, Kodaira, Tokyo 187–8502, Japan and [b]Core Research for Evolutional Science and Technology (CREST) of Japan Science and Technology Corporation, 4–1–8 Honcho, Kawaguchi-shi, Saitama 332–0012, Japan

(Received April 9, 2003)

Prion protein (PrP) exists in two different isoforms; a normal cellular isoform (PrP^C) and an abnormal infectious isoform (PrP^{Sc}), the latter is a causative agent of prion disease such as Bovine Spongiform Encephalopathy (BSE, mad cow disease) and Creutzfeldt-Jakob disease (CJD). Great concern about variant CJD, which is caused by ingesting BSE-contaminated products, is also emerging and spreading over Japan since the first BSE-affected cattle was identified in September, 2001. The amino acid sequences of PrP^C and PrP^{Sc} are identical, but their conformations are rather different; PrP^C is rich in the non β-sheet isoform while PrP^{Sc} is rich in the β-sheet isoform. Our prion research focuses on further understanding such an unprecedented mechanism by identifying auxiliary factor(s) other than PrP^C and PrP^{Sc}. These studies also help us to develop "therapeutics and prevention methods" for prion disease. Three major trials; genetic manipulation with dominant negative mutant PrP^C gene working against a hypothetical host-specific factor, antibody therapy with anti-PrP antibodies which block PrP^C-PrP^{Sc} binding, and PrP^{Sc} unfolding therapy with a novel-class molecular chaperone, are currently underway.

Key words —— prion protein, prion disease, dominant negatives, anti-prion protein antibody, molecular chaperone

Prions and Prion Disease

Many lines of evidence have argued persuasively that prions are composed largely, if not exclusively, of the scrapie isoform of prion protein (PrP). An abnormally folded isoform (PrP^{Sc}) of the normal, cellular prion protein (PrP^C) stimulates the conversion of PrP^C into nascent PrP^{Sc} in prion diseases (Fig. 1). The accumulation of PrP^{Sc} leads to neuronal death followed by central nervous system (CNS) dysfunction.[1] The discovery that mutations in the PrP gene cause inherited prion disease in humans,[2] which is transmissible to laboratory animals,[3] and the generation of infectious prions in transgenic (Tg) mice expressing mutant PrP assert that prions are devoid of nucleic acid.[4,5] It is be also important to mention that we identified a 55-residue peptide of a mutant prion protein that can be refolded into at least two distinct conformations.[6] When inoculated intracerebrally into the appropriate transgenic mouse host, 20 of 20 mice receiving the β-form of this peptide developed signs of CNS dysfunction at ~360 days, with neurohistologic changes that are pathognomonic of Gerstmann-Sträussler-Scheinker (GSS) disease.[7] By contrast, 8 of 8 mice receiving a non-β-form of the peptide failed to develop any neuropathologic changes more than 600 days after the peptide injections. Thus, a chemically synthesized peptide refolded into the appropriate conformation can accelerate or possibly initiate prion disease.

That the cellular isoform of PrP^C interacts with PrP^{Sc} during the formation of nascent PrP^{Sc} was surmised from Tg mouse studies where mice expressing a Syrian hamster (SHa) PrP transgene were susceptible to SHa prions.[8] When similar Tg mice were produced expressing human (Hu) PrP, no transmission of Hu prions was found. However, mice expressing a chimeric Hu-mouse PrP (Hu-MoPrP) transgene denoted MHu2M were susceptible to Hu prions. In addition, we found that Tg mice expressing HuPrP did become susceptible to Hu prions when they were crossed with PrP-deficient ($Prnp^{0/0}$) mice. Studies on the transmission of Hu prions to Tg mice

*To whom correspondence should be addressed: Department of Cortical Function Disorders, National Institute of Neuroscience, National Center of Neurology and Psychiatry, 4–1–1 Ogawahigashi, Kodaira, Tokyo 187–8502, Japan. Tel.: +81-42-346-1718; Fax: +81-42-346-1748; E-mail: kaneko@ncnp.go.jp

suggested that another molecule provisionally designated protein X participates in the formation of nascent PrP^{Sc} [3] (Fig. 2). We report the identification of the site at which protein X binds to PrP^{C} using scrapie-infected Mo neuroblastoma cells transfected with chimeric Hu-MoPrP genes even though protein X has not yet been isolated. Substitution of a Hu residue at position 214 or 218 prevented PrP^{Sc} formation.[9] The side chains of these residues protrude from the same surface of the C-terminal α-helix and form a discontinuous epitope with residues 167 and 171 in an adjacent loop (Fig. 3).

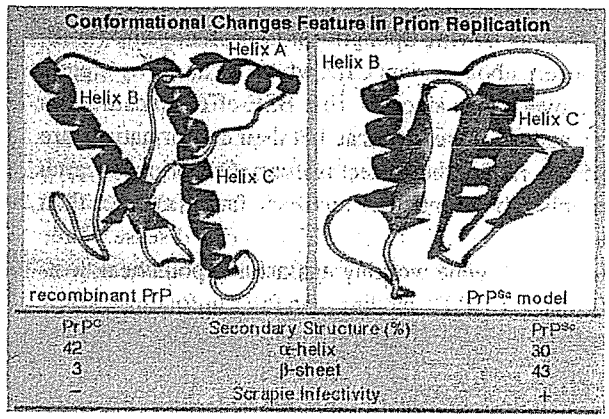

Fig. 1. Two Isoforms of PrP

PrP^{C} represents normal cellular isoform of PrP, and PrP^{Sc} represents abnormal disease isoform of PrP.

Therapeutic Approaches in Prion Disease

At present, there is no accepted therapy for prion diseases, and whether the drug quinacrine will prove to be effective in treating these diseases remains to be established.[10] In addition to quinacrine,[11] other compounds that block prion replication as well as stimulate the clearance of existing prions include branched polyamines,[12] phthalocyanines and porphyrin derivatives,[13] Congo red,[14] compound 60,[15] β-breaker peptides,[16] and anti-PrP antibodies.[17,18] Although many of the foregoing compounds are able to clear prions in scrapie-infected neuroblastoma cells, none have been shown to be effective in animals or humans to date. It is noteworthy that both vaccination and passive immunization have effectively decreased Aβ amyloid deposits in the brains of Tg mice expressing mutant amyloid precursor protein. Unfortunately, some attempts to vaccinate humans with Aβ have resulted in allergic meningoencephalitis, which halted the clinical trial.[19]

1. Dominant Negative PrP

One compound was designed to mimic dominant negative inhibition of prion replication.[15] Dominant-negative inhibition occurs when the product of the mutant or variant allele interferes with a func-

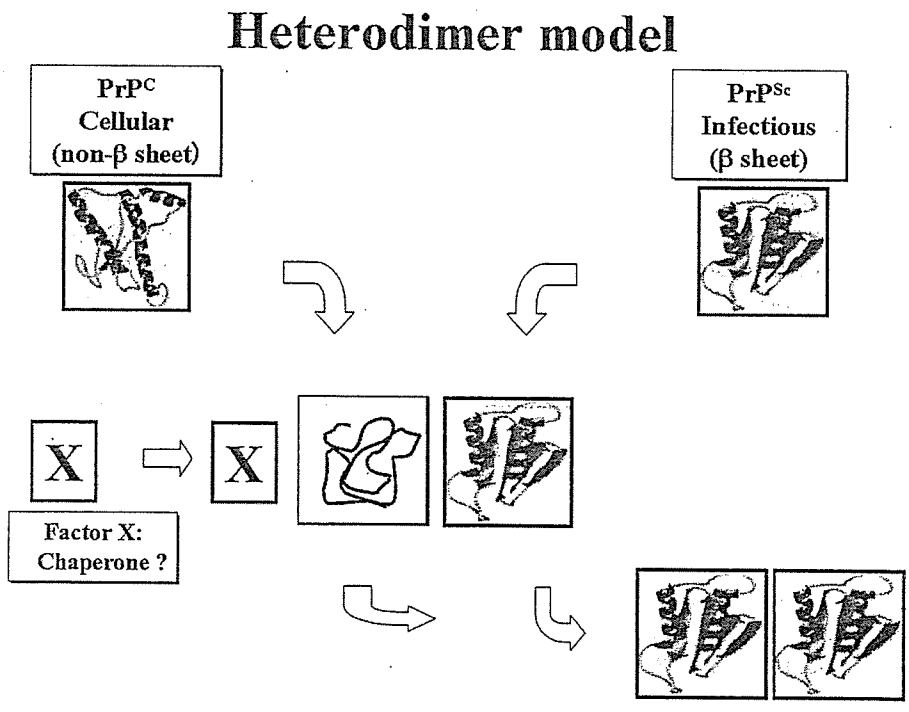

Fig. 2. Heterodimer Model of PrP^{Sc} Replication

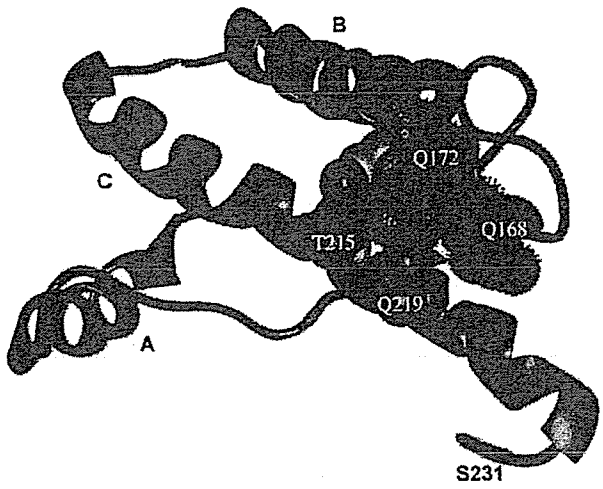

Fig. 3. Hypothetical Molecular Chaperone (Protein X) Binding Site on PrP^C

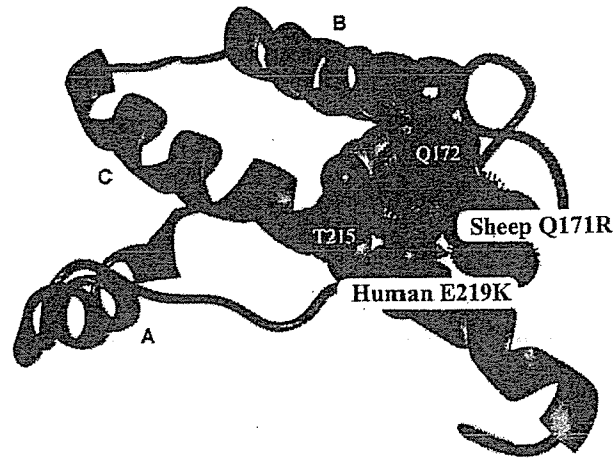

Fig. 4. Two Sheep and Human Polymorphisms Resistant to PrP^{Sc} by Exhibiting a Dominant Negative Effect

tion of the wild-type (wt) allelic protein. Naturally occurring polymorphic variants of PrP, and Q171R and E219K, which are known to render sheep and humans resistant to scrapie and CJD,[20,21] were found to act as dominant negatives in scrapie-infected neuroblastoma cells[9,22] (Fig. 4).

Based on these findings, we undertook studies on dominant negative PrP. To determine whether dominant-negative inhibition occurs *in vivo*, we produced Tg mice expressing PrP with either the Q167R or Q218K mutation alone or in combination with wt PrP.[23] Tg(MoPrP,Q167R)$Prnp^{0/0}$ mice expressing mutant PrP at levels equal to non-Tg mice remained healthy for > 550 days, indicating that inoculation with prions did not cause disease. Immunoblots of brain homogenates and histological analysis did not reveal abnormalities. Tg(MoPrP,Q167R)$Prnp^{+/+}$ mice expressing both mutant and wt PrP did not exhibit neurological dysfunction, but their brains revealed low levels of PrP^{Sc}, and sections showed numerous vacuoles and severe astrocytic gliosis at 300 days after inoculation. Both Tg(MoPrP, Q218K)$Prnp^{0/0}$ and Tg(MoPrP,Q218K)$Prnp^{+/+}$ mice expressing high levels of the transgene product remained healthy for > 300 days after inoculation. Neither PrP^{Sc} nor neuropathologic changes were found.

The inability of MoPrP(Q167R) and MoPrP(Q218K) to support prion replication raises the possibility of producing prion-resistant animals that express PrP with a single amino acid substitution. Because sheep homozygous for R at position 171 already exist, breeding populations of resistant sheep is a reasonable approach. Presumably, this was the genetic basis of Parry's scrapie eradication program in Great Britain 40 years ago.[24] A similar approach, inoculating Tg(BoPrP,Q179R) or Tg(BoPrP,Q230K) mice with bovine prions might be useful in evaluating the utility of producing prion-resistant cattle. Although the introduction of a point mutation may not produce complete resistance to prion infection as disruption of the *Prnp* gene does,[25,26] it may prove to be more desirable to utilize such amino acid substitutions since they are natural polymorphisms in humans and sheep.

2. Anti-PrP Antibodies

Reagents specifically binding either PrP conformer may interrupt prion production by inhibiting this interaction. We examined the ability of several recombinant antibody antigen-binding fragments (Fabs) to inhibit prion propagation in cultured mouse neuroblastoma cells (ScN2a) infected with PrP^{Sc}. We showed that antibodies binding cell-surface PrP^C inhibit PrP^{Sc} formation in a dose-dependent manner[17] (Fig. 5). In cells treated with the most potent antibody, Fab D18, prion replication is abolished and pre-existing PrP^{Sc} is rapidly cleared, suggesting that this antibody may cure an established infection. The potent activity of Fab D18 is associated with its ability to better recognize the total population of PrP^C molecules on the cell surface, and with the location of its epitope on PrP^C. Our observations support the use of antibodies in the prevention and treatment of prion diseases and identify a region of PrP^C for drug targeting.

For *in vivo* applications, Fab fragments have the disadvantage of a short half-life, and may not efficiently traverse from the peripheral circulation into the central nervous system. Whole-antibody molecules prepared from the Fabs will probably be more useful, but may require engineering to prevent the recruitment of an immunological effect to antibody-coated cells.[27]

3. PrP^{Sc} Unfolding Biomolecules

Polypeptide chains are synthesized inside cells as linear molecules and then must be folded into functional structures to perform catalysis. The failure of polypeptides to adopt their proper structure is a major threat to cell function and viability. Therefore, chaperones like HSP70s family proteins that are located in every cellular compartment, bind a wide range of proteins, and play an essential role in protein folding machinery or preventing misfolding and aggregation of newly synthesized or unfolded proteins. Recently we found and isolated novel protein unfolding activity in *S. cerevisiae* (N.S.H. paper in preparation). This activity is ATP-dependent and moreover does not have any specificity *in vitro*. Interestingly, the activity unfolded the prion protein structure even though it included a β-sheet structure, α-synulein, and amloid β-peptide (1–42) (Fig. 6). By adding specificity to the activity, it may become a powerful tool as a novel therapeutic approach for aggregation diseases by dissolving such aggregates.

We have also explored chaperone activities related to the conformational transition of PrP^{C} into PrP^{Sc} in mammalian cells. We have attempted to identify activities which modulate the conformation of PrP^{C} in mouse neuroblastoma cells using a trypsin-sensitivity assay by which we identified the yeast protein unfolding activity as mentioned above. As a result, we obtained activities which modulated recombinant PrP conformation in nuclear, microsome, and cytosol fractions.

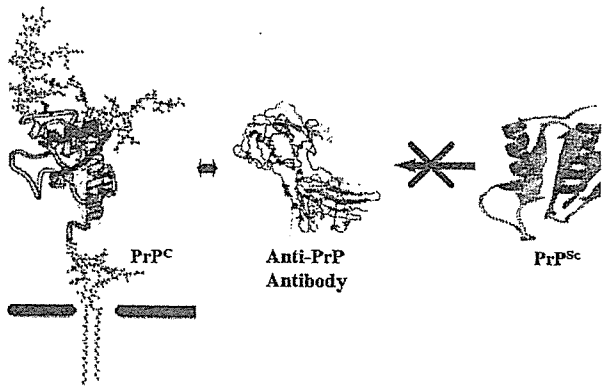

Fig. 5. Inhibition of the PrP^{C}-PrP^{Sc} Interaction by Anti-PrP Antibody

4. New Therapeutic Approach in Neurodegenerative Disorders

As it has been shown in past therapeutics approaches for other major human diseases such as cancer or HIV infection, a combination therapy will also be considered for neurodegenerative disorders in the near future. Even if each therapeutic approach exhibits a limited cure with considerable adverse effects, a combination of two or three approaches might be able to improve the patient's prognosis.

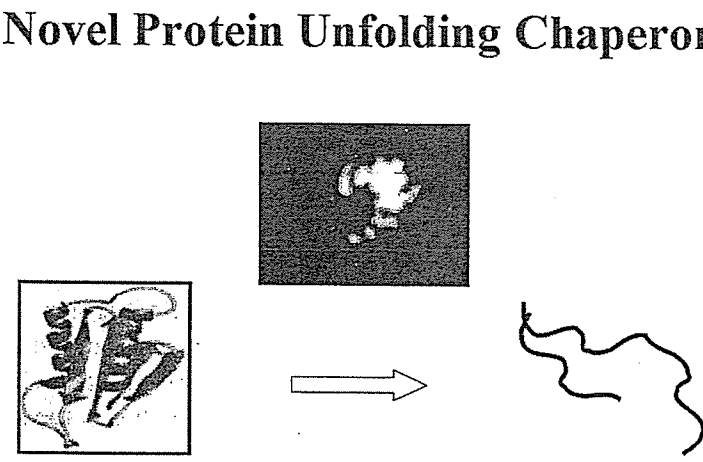

Fig. 6. A Novel Unfolding Chaperone Might Inactivate PrP^{Sc}

Whether the combination of drugs and biomolecules such as low-dose quinacrine, dominant negative PrP, anti-PrP antibody, and a PrP^{Sc}-unfolding chaperone more efficiently inhibits prion replication remains to be established. Such studies are currently underway.

Acknowledgements We thank Dr. Stanley B. Prusiner and his co-workers at the Institute for Neurodegenerative Diseases, the University of California, San Francisco and the Department of Immunology, Scripps Institute of Technology for their supports. This work was supported by grants-in-aids from the Ministry of Health, Labor and Welfare, the Ministry of Education and Science, and Core Research for Evolutional Science and Technology (CREST) of Japan Science and Technology Corporation.

REFERENCES

1) DeArmond, S. J., Mobley, W. C., DeMott, D. L., Barry, R. A., Beckstead, J. H. and Prusiner, S. B. (1987) Changes in the localization of brain prion proteins during scrapie infection. *Neurology*, **37**, 1271–1280.
2) Hsiao, K., Baker, H. F., Crow, T. J., Poulter, M., Owen, F., Terwilliger, J. D., Westaway, D., Ott, J. and Prusiner, S. B. (1989) Linkage of a prion protein missense variant to Gerstmann-Strossler syndrome. *Nature* (London), **338**, 342–345.
3) Telling, G. C., Scott, M., Mastrianni, J., Gabizon, R., Torchia, M., Cohen, F. E., DeArmond, S. J. and Prusiner, S. B. (1995) Prion propagation in mice expressing human and chimeric PrP transgenes implicates the interaction of cellular PrP with another protein. *Cell*, **83**, 79–90.
4) Hsiao, K. K., Scott, M., Foster, D., Groth, D. F., DeArmond, S. J. and Prusiner, S. B. (1990) Spontaneous neurodegeneration in transgenic mice with mutant prion protein. *Science*, **250**, 1587–1590.
5) Telling, G. C., Haga, T., Torchia, M., Tremblay, P., DeArmond, S. J. and Prusiner, S. B. (1996) Interactions between wild-type and mutant prion proteins modulate neurodegeneration in transgenic mice. *Genes Dev.*, **10**, 1736–1750.
6) Kaneko, K., Wille, H., Mehlhorn, I., Zhang, H., Ball, H., Cohen, F. E., Baldwin, M. A. and Prusiner, S. B. (1997) Molecular properties of complexes formed between the prion protein and synthetic peptides. *J. Mol. Biol.*, **270**, 574–586.
7) Kaneko, K., Ball, H. L., Wille, H., Zhang, H., Groth, D., Torchia, M., Tremblay, P., Safar, J., Prusiner, S. B., DeArmond, S. J., Baldwin, M. A. and Cohen, F. E. (2000) A synthetic peptide initiates Gerstmann-Straussler-Scheinker (GSS) Disease in transgenic mice. Running title: A peptide causes Gerstmann-Straussler-Scheinker disease. *J. Mol. Biol.*, **295**, 997–1007.
8) Prusiner, S. B., Scott, M., Foster, D., Pan, K.-M., Groth, D., Mirenda, C., Torchia, M., Yang, S.-L., Serban, D., Carlson, G. A., Hoppe, P. C., Westaway, D. and DeArmond, S. J. (1990) Transgenetic studies implicate interactions between homologous PrP isoforms in scrapie prion replication. *Cell*, **63**, 673–686.
9) Kaneko, K., Zulianello, L., Scott, M., Cooper, C. M., Wallace, A. C., James, T. L., Cohen, F. E. and Prusiner, S. B. (1997) Evidence for protein X binding to a discontinuous epitope on the cellular prion protein during scrapie prion propagation. *Proc. Natl. Acad. Sci. U.S.A.*, **94**, 10069–10074.
10) Korth, C., May, B. C. H., Cohen, F. E. and Prusiner, S. B. (2001) Acridine and phenothiazine derivatives as pharmacotherapeutics for prion disease. *Proc. Natl. Acad. Sci. U.S.A.*, **98**, 9836–9841.
11) Doh-Ura, K., Iwaki, T. and Caughey, B. (2000) Lysosomotropic agents and cysteine protease inhibitors inhibit scrapie- associated prion protein accumulation. *J. Virol.*, **74**, 4894–4897.
12) Supattapone, S., Nguyen, H. O., Cohen, F. E., Prusiner, S. B. and Scott, M. R. (1999) Elimination of prions by branched polyamines and implications for therapeutics. *Proc. Natl. Acad. Sci. U.S.A.*, **96**, 14529–14534.
13) Caughey, W. S., Raymond, L. D., Horiuchi, M. and Caughey, B. (1998) Inhibition of protease-resistant prion protein formation by porphyrins and phthalocyanines. *Proc. Natl. Acad. Sci. U.S.A.*, **95**, 12117–12122.
14) Demaimay, R., Harper, J., Gordon, H., Weaver, D., Chesebro, B. and Caughey, B. (1998) Structural aspects of Congo red as an inhibitor of protease-resistant prion protein formation. *J. Neurochem.*, **71**, 2534–2541.
15) Perrier, V., Wallace, A., Kaneko, K., Safar, J., Prusiner, S. B. and Cohen, F. E. (2000) Mimicking dominant negative inhibition of prion replication through structure-based drug design. *Proc. Natl. Acad. Sci. U.S.A.*, **97**, 6073–6078.
16) Soto, C., Kascsak, R. J., Saborio, G. P., Aucouturier, P., Wisniewski, T., Prelli, F., Kascsak, R., Mendez, E., Harris, D. A., Ironside, J., Tagliavini, F., Carp, R. I. and Frangione, B. (2000) Reversion of prion protein conformational changes by synthetic beta-sheet breaker peptides. *Lancet*, **355**, 192–197.

17) Peretz, D., Williamson, R. A., Kaneko, K., Vergara, J., Leclerc, E., Schmitt-Ulms, G., Mehlhorn, I. R., Legname, G., Wormald, M. R., Rudd, P. M., Dwek, R. A., Burton, D. R. and Prusiner, S. B. (2001) Antibodies inhibit prion propagation and clear cell cultures of prion infectivity. *Nature* (London), **412**, 739–743.
18) Enari, M., Flechsig, E. and Weissmann, C. (2001) Scrapie prion protein accumulation by scrapie-infected neuroblastoma cells abrogated by exposure to a prion protein antibody. *Proc. Natl. Acad. Sci. U.S.A.*, **98**, 9295–9299.
19) Birmingham, K. and Frantz, S. (2002) Setback to Alzheimer vaccine studies. *Nat. Med.*, **8**, 199–200.
20) Westaway, D., Zuliani, V., Cooper, C. M., Da Costa, M., Neuman, S., Jenny, A. L., Detwiler, L. and Prusiner, S. B. (1994) Homozygosity for prion protein alleles encoding glutamine-171 renders sheep susceptible to natural scrapie. *Genes Dev.*, **8**, 959–969.
21) Shibuya, S., Higuchi, J., Shin, R. W., Tateishi, J. and Kitamoto, T. (1998) Protective prion protein polymorphisms against sporadic Creutzfeldt-Jakob disease [letter]. *Lancet*, **351**, 419.
22) Zulianello, L., Kaneko, K., Scott, M., Erpel, S., Han, D., Cohen, F. E. and Prusiner, S. B. (2000) Dominant-negative inhibition of prion formation diminished by deletion mutagenesis of the prion protein. *J. Virol.*, **74**, 4351–4360.
23) Perrier, V., Kaneko, K., Safar, J., Vergara, J., Tremblay, P., DeArmond, S. J., Cohen, F. E., Prusiner, S. B. and Wallace, A. C. (2002) Dominant-negative inhibition of prion replication in transgenic mice. *Proc. Natl. Acad. Sci. U.S.A.*, **99**, 13079–13084.
24) Parry, H. B. (1962) Scrapie: a transmissible and hereditary disease of sheep. *Heredity*, **17**, 75–105.
25) Bueler, H., Aguzzi, A., Sailer, A., Greiner, R.-A., Autenried, P., Aguet, M. and Weissmann, C. (1993) Mice devoid of PrP are resistant to scrapie. *Cell*, **73**, 1339–1347.
26) Prusiner, S. B., Groth, D., Serban, A., Stahl, N. and Gabizon, R. (1993) Attempts to restore scrapie prion infectivity after exposure to protein denaturants. *Proc. Natl. Acad. Sci. U.S.A.*, **90**, 2793–2797.
27) Idusogie, E. E., Presta, L. G., Gazzano-Santoro, H., Totpal, K., Wong, P. Y., Ultsch, M., Meng, Y. G. and Mulkerrin, M. G. (2000) Mapping of the C1q binding site on rituxan, a chimeric antibody with a human IgG1 Fc. *J. Immunol.*, **164**, 4178–4184.

Small GTPase Rin induces neurite outgrowth through Rac/Cdc42 and calmodulin in PC12 cells

Mitsunobu Hoshino and Shun Nakamura

Division of Biochemistry and Cellular Biology, National Institute of Neuroscience, National Center of Neurology and Psychiatry, Tokyo 187-8502, Japan

The novel Ras-like small GTPase Rin is expressed prominently in adult neurons, and binds calmodulin (CaM) through its COOH-terminal–binding motif. It might be involved in calcium/CaM-mediated neuronal signaling, but Rin-mediated signal transduction pathways have not yet been elucidated. Here, we show that expression of Rin induces neurite outgrowth without nerve growth factor or mitogen-activated protein kinase activation in rat pheochromocytoma PC12 cells. Rin-induced neurite outgrowth was markedly inhibited by coexpression with dominant negative Rac/Cdc42 protein or CaM inhibitor treatment. We also found that expression of Rin elevated the endogenous Rac/Cdc42 activity. Rin mutant proteins, in which the mutation disrupted association with CaM, failed to induce neurite outgrowth irrespective of Rac/Cdc42 activation. Disruption of endogenous Rin function inhibited the neurite outgrowth stimulated by forskolin and extracellular calcium entry through voltage-dependent calcium channel evoked by KCl. These findings suggest that Rin-mediated neurite outgrowth signaling requires not only endogenous Rac/Cdc42 activation but also Rin–CaM association, and that endogenous Rin is involved in calcium/CaM-mediated neuronal signaling pathways.

Introduction

The Ras superfamily small GTPases link cell surface receptors to intracellular signal transduction pathways that regulate cell growth and differentiation (Kaziro et al., 1991). The Ras protein functions as a molecular switch by cycling from the inactive GDP-bound state to the active GTP-bound state (Kaziro et al., 1991; Bos, 1998). Activation of the Ras requires several guanine nucleotide exchange factors (GEFs) which induce the dissociation of GDP to allow GTP association (Bos, 1998; Vojtek and Der, 1998; Reuther and Der, 2000). On the other hand, GTPase-activating proteins (GAPs) accelerate the rate of intrinsic GTPase activities of the Ras and inactivate its biological activities (Bos, 1998; Vojtek and Der, 1998; Reuther and Der, 2000). Through its G2 effector region that is involved in the binding of specific target proteins, the activated GTP-bound Ras interacts with target proteins, such as serine/threonine kinase Raf-1, the p110 catalytic subunit of phosphatidylinositol 3-kinase (PI3K), the exchange factor for Ral GTPase protein RalGDS, and so on (Bos, 1998; Vojtek and Der, 1998).

The newly discovered GTPase, Rin, and its *Drosophila* homologue Ric have been classified into the Ras superfamily (Lee et al., 1996; Wes et al., 1996; Shao et al., 1999; Reuther and Der, 2000). Rin binds GTP in vitro and exhibits an intrinsic GTPase activity (Lee et al., 1996; Shao et al., 1999). Rin shares a high sequence identity with the Ras and has a highly conserved but distinct G2 effector region (HDPTIEDAY) in which histidine is substituted for tyrosine at position 32, and alanine is substituted for serine at position 39 (Lee et al., 1996). Moreover, Rin displays unique characteristics that are not observed in other members of the Ras superfamily, such as CaM-binding activity and the lack of a typical COOH-terminal prenylation motif (CAAX motif) required for membrane association (Lee et al., 1996). Rin is expressed only in neurons and binds CaM in a calcium-dependent manner (Lee et al., 1996). The expression of Rin is more prominent in the adult brain than in the brain at earlier stages (Lee et al., 1996). We demonstrated previously that Rin is activated by growth factor stimulation using a Rin pull-down assay system (Hoshino and Nakamura,

Address correspondence to Mitsunobu Hoshino, Division of Biochemistry and Cellular Biology, National Institute of Neuroscience, National Center of Neurology and Psychiatry, 4-1-1, Ogawahigashi, Kodaira, Tokyo 187-8502, Japan. Tel.: 81-42-346-1722. Fax: 81-42-346-1752. email: hoshinom@ncnp.go.jp

Key words: calcium; MAPK; Ras; Rho

Abbreviations used in this paper: CaMK, calcium/CaM-dependent protein kinase; CRIB, Cdc42/Rac interactive binding; GAP, GTPase-activating protein; GEF, guanine nucleotide exchange factor; LPA, lysophosphatidic acid; PAK, p21-activated kinase; PI3K, phosphatidylinositol 3-kinase; siRNA, short interfering RNA.

The Journal of Cell Biology, Volume 163, Number 5, December 8, 2003 1067–1076
http://www.jcb.org/cgi/doi/10.1083/jcb.200308070

2002). These studies raised the possibility that Rin plays important roles in the control of the calcium/CaM-mediated signaling pathways in the nervous system. To date, however, few of the intracellular functions and signal transduction pathways of Rin have been characterized.

Rat pheochromocytoma cell line PC12 cells are a useful model system for examining mechanisms of neuronal differentiation and signal transduction (Greene and Tischler, 1976). They differentiate in response to NGF with growth arrest and show neurite outgrowth resembling that of sympathetic neurons (Greene and Tischler, 1976). After NGF stimulation, a number of signal transduction pathways in PC12 cells are activated, including the Trk receptor tyrosine kinase–Ras-MAPK cascade (Kaplan and Stephens, 1994). It has been shown that sustained MAPK activation is necessary for NGF-induced neurite outgrowth in PC12 cells (Marshall, 1995).

The Rho GTPase family proteins, which consist of the closely related GTPases Rho, Rac, and Cdc42, participate in the actin cytoskeleton dynamics, reactive oxygen generation, and tumorigenesis (Lim et al., 1996; Bishop and Hall, 2000). In Swiss 3T3 fibroblasts, Rho regulates growth factor–stimulated stress fiber formation, whereas Rac and Cdc42 regulate growth factor–stimulated membrane ruffling and filopodium formation, respectively (Lim et al., 1996; Bishop and Hall, 2000). To date, many Rho family effector proteins have been identified. For example, the GTP-bound Rho can bind to the Rho-associated coiled-coil–forming kinases, whereas the GTP-bound Rac and Cdc42 can bind to the p21-activated kinases (PAKs) through their Cdc42/Rac interactive binding (CRIB) domain, and these kinases control the regulation of the actin cytoskeleton system (Lim et al., 1996; Bishop and Hall, 2000).

CaM is a ubiquitous, highly conserved protein and is recognized as a major calcium sensor for diverse intracellular enzymes (Rhoads and Friedberg, 1997). When cells are responding to an increase in the intracellular calcium concentration, CaM undergoes a conformational change, binds to its target proteins, and evokes many cellular processes, including cell cycle regulation, cytoskeletal organization, and ion channel regulation (Rhoads and Friedberg, 1997).

Here, we examined the role of Rin in neuronal signaling, especially focusing on the formation and morphology of neurite processes in calcium/CaM-mediated signaling pathway. Our results showed that the expression of Rin induced neurite outgrowth without NGF stimulation or MAPK activation, and this phenomenon was markedly inhibited by coexpression with the dominant negative Rac/Cdc42 protein or treatment with CaM inhibitor. We also found that Rin proteins activated endogenous Rac/Cdc42 proteins and that Rin-induced neurite outgrowth required Rin association with CaM. Moreover, we show that endogenous Rin proteins are involved in calcium-mediated neurite outgrowth and propose that they play pivotal roles in regulating neuronal signaling pathways.

Results

Neurite outgrowth in Rin-transfected PC12 cells

To elucidate whether Rin protein is involved in neuronal differentiation, Myc epitope-tagged wild-type Rin or constitutively active Rin mutant (Q78L; Gln78 was replaced with Leu) was transiently expressed into PC12 cells. The cognate Q61L mutant in Ras protein is regarded as a constitutively active mutant (Vojtek and Der, 1998). As shown in Fig. 1 A, transfection of PC12 cells with a control plasmid (pEF-Bos empty vector) resulted in cells with a rounded morphology like that of untransfected cells. However, transfection of the wild-type Rin protein resulted in cells showing neurite outgrowth in the absence of NGF (Fig. 1 B). Constitutively active RinQ78L protein also induced neurite outgrowth in

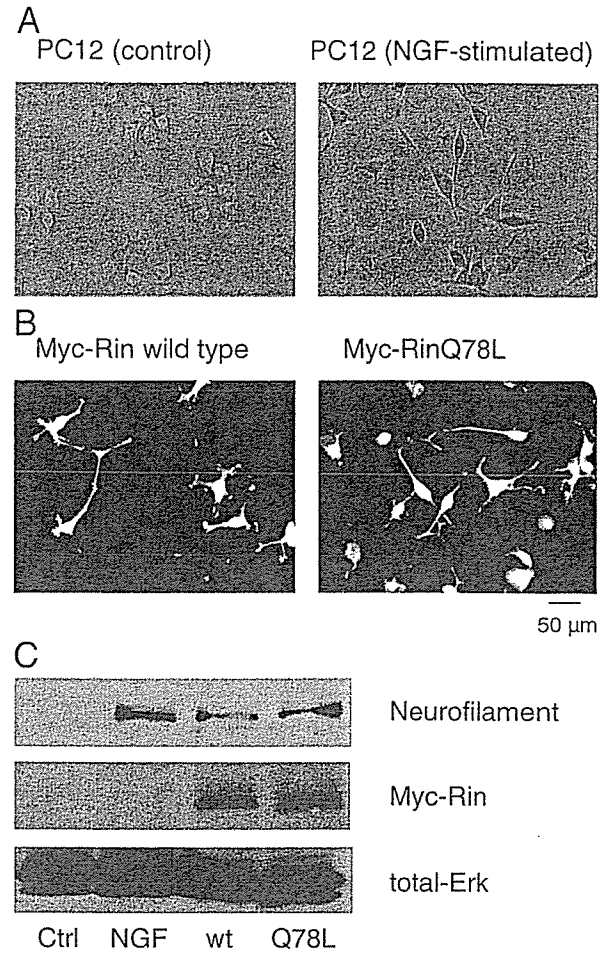

Figure 1. **Rin protein induces neurite outgrowth in PC12 cells.** (A) Empty vector–transfected PC12 cells were left untreated or stimulated with 50 ng/ml NGF for 44 h. Cells were fixed with 3% PFA-PBS and were visualized under a phase contrasted bright field microscopy. (B) PC12 cells were transfected with an expression vector encoding Myc-tagged wild-type Rin or Myc-tagged constitutively active RinQ78L protein. After 48 h, transfected cells were fixed, permeabilized, and processed for immunofluorescence with an anti-Myc antibody. Transfected cells were visualized with a Cy3-labeled anti–mouse secondary antibody. (C) PC12 cells were left untreated or stimulated with 50 ng/ml NGF for 2 d. Other PC12 cells were transfected with an expression vector encoding Myc-tagged wild-type Rin or Myc-tagged RinQ78L protein and were maintained for 5 d. Cells were washed with an ice-cold PBS buffer and lysed with an ice-cold lysis buffer. Cell lysates were cleared by centrifugation and Western blotting was performed as described in the Materials and methods, using an antineurofilament antibody, an anti-MAPK 1/2 antibody, and an anti-Myc antibody. Data are representative of three independent experiments, which gave essentially identical results.

Table I. Rin-induced neurites and NGF-induced neurites in PC12 cells

	Rin-induced neurites[a]	NGF-induced neurites[b]
Total neurite length per cell (μm)	101.34 ± 5.53	81.33 ± 4.35
No. of primary processes originating from somata	3.10 ± 0.11	2.14 ± 0.10
No. of branching points per cell	2.31 ± 0.17	0.15 ± 0.05

PC12 cells were stimulated with 50 ng/ml NGF for 2 d or were transfected with a Myc-tagged wild-type Rin protein vector and maintained for 2 d. Cells were fixed, immunostained with an anti-Myc antibody, and observed by microscopy. Means ± SEM are shown.
[a] $n = 112$.
[b] $n = 108$.

PC12 cells (Fig. 1 B). NGF-induced neurites showed linear extensions and few branchings (Fig. 1 A), whereas Rin-transfected cells showed multiple neurites per cell and plenty of branchings (Fig. 1 B and Table I). The multiple neurites and profuse branchings were also observed when HA-tagged Rin protein was expressed instead of Myc-Rin protein or when anti-Rin antibody was used as a primary antibody instead of anti-Myc epitope tag antibody (unpublished data).

To examine whether this biological effect of Rin protein is related to the neuronal differentiation, we assessed an expression of a differentiation-associated marker protein neurofilament. Neurofilament is an intermediate filament expressed specifically in neurons and NGF is known to increase the levels of neurofilament proteins in PC12 cells (Lindenbaum et al., 1988). As shown in Fig. 1 C, the increase in neurofilament levels was observed in Rin-transfected cells as well as in NGF-treated cells, whereas the expression level of MAPK remains constant. Neurofilament proteins are barely visible in the control PC12 cell extracts (Fig. 1 C). These results suggest that Rin protein induces neuronal differentiation, at least in terms of the induction of neurofilament expression.

Rin-mediated neurite outgrowth is MAPK pathway independent

It has been well established that the MAPK cascade is necessary for neuronal differentiation of PC12 cells (Kaplan and Stephens, 1994). We examined the activity of MAPK in Rin-expressing cells by Western blot analysis using antiphospho-MAPK antibody. As shown in Fig. 2 A, Rin-transfected cells did not show obvious MAPK activation. Moreover, pretreatment with 7.5 μM U0126 (a MAPK kinase inhibitor), which concentration is sufficient for the inhibition of MAPK activity after 50 ng/ml NGF stimulation (Fig. 2 B) and of NGF-induced neurite outgrowth (Fig. 2 C), did not affect the Rin-mediated neurite outgrowth in PC12 cells (Fig. 2 C). These data suggest that the MAPK pathway is not likely to be responsible for the Rin-mediated neurite outgrowth.

Rin-mediated neurite outgrowth is inhibited by dominant negative Rac/Cdc42

To determine whether Rin-mediated neurite outgrowth was dependent on the activity of Rho family GTPase protein,

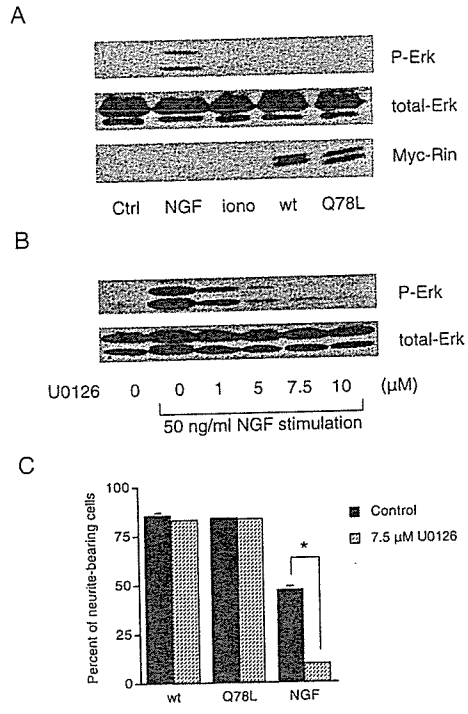

Figure 2. **MAPK is not involved in the Rin-signaling pathway in PC12 cells.** (A) PC12 cells were serum starved for 24 h and left untreated or stimulated with 50 ng/ml NGF or 0.5 μg/ml ionomycin for 5 min. Other PC12 cells were transfected with an expression vector encoding Myc-tagged wild-type Rin or Myc-tagged RinQ78L protein and serum starved for 24 h. Cell lysates were subjected to Western blotting as described in the Materials and methods, using an antiphospho-MAPK antibody, an anti-MAPK 1/2 antibody and an anti-Myc antibody. Data are representative of three independent experiments, which gave essentially identical results. (B) Serum-starved PC12 cells were preincubated with vehicle or various amounts of MAPK kinase inhibitor U0126 for 48 h at 37°C, followed by 50 ng/ml NGF for 5 min. Cell lysates were subjected to Western blotting as described in the Materials and methods. Data are representative of three independent experiments, which gave essentially identical results. (C) Rin-transfected cells or 50 ng/ml NGF-stimulated cells were treated with vehicle or 7.5 μM U0126 for 48 h at 37°C. Cells were fixed and visualized with an anti-Myc antibody. Cells with neurites exceeding one cell body diameter in length were counted as a ratio of the total number of transfected cells. Columns and vertical bars denote the mean ± SEM, respectively ($n = 3$). Asterisk indicates $P < 0.05$ as compared with the control value.

we cotransfected cells with wild-type Rin and dominant negative Rac1 (RacS17N) proteins. As shown in Fig. 3 A, RacS17N suppressed the Rin-mediated neurite outgrowth completely. Dominant negative Cdc42 (Cdc42S17N) protein also suppressed it completely (Fig. 3, A and B). In contrast, dominant negative RhoA (RhoT19N) protein suppressed it only partially (Fig. 3 B).

Endogenous Rac/Cdc42 activation is required for Rin-mediated neurite outgrowth

To examine whether the Rac/Cdc42 activity is required as a downstream signaling component of Rin protein, we measured the amount of GTP-bound Rac/Cdc42 in Rin-transfected cells using a pull-down assay. This assay system makes use of the CRIB domain of PAK as a GST fusion protein,

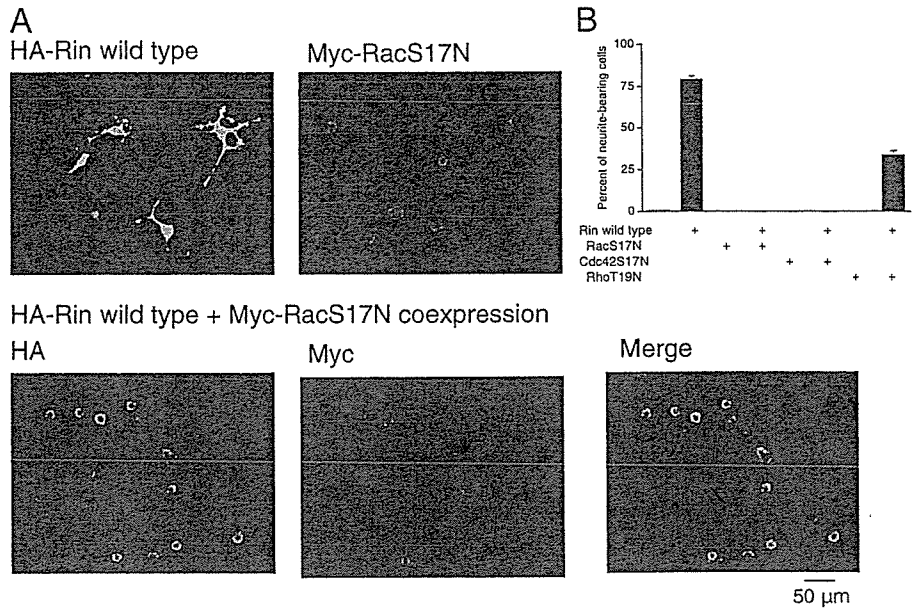

Figure 3. **Dominant negative Rac/Cdc42 inhibits the Rin-mediated neurite outgrowth in PC12 cells.** (A and B) Cells were transfected with an HA-tagged wild-type Rin vector and a Myc-tagged dominant negative RacS17N/Cdc42S17N/RhoT19N vector either alone or in pairs. After 48 h, cells were fixed and immunostained with an anti-HA antibody and an anti-Myc antibody. Columns and vertical bars denote the mean ± SEM, respectively ($n = 3$). In the merge of A, HA-Rin staining is shown in green (using FITC-labeled anti–rat secondary antibody), whereas Myc-Rac staining is shown in red (using Cy3-labeled anti–mouse secondary antibody).

which specifically binds to and isolates the GTP-bound Rac/Cdc42 (Benard et al., 1999). Transient expression of Rin in PC12 cells resulted in an obvious increase of the amounts of GTP-bound Rac/Cdc42 protein (Fig. 4, lane 2), when compared with the empty vector–transfected cells (Fig. 4, lane 1). The level of this activation was similar to the NGF-induced Rac/Cdc42 activation (Fig. 4, lane 7). RinQ78L protein also evoked the endogenous Rac/Cdc42 activation to the same degree as the wild-type did (Fig. 4, lane 3). These data suggest that Rac/Cdc42 is located in the downstream signaling pathway of Rin and that Rin-mediated neurite outgrowth requires endogenous Rac/Cdc42 activity.

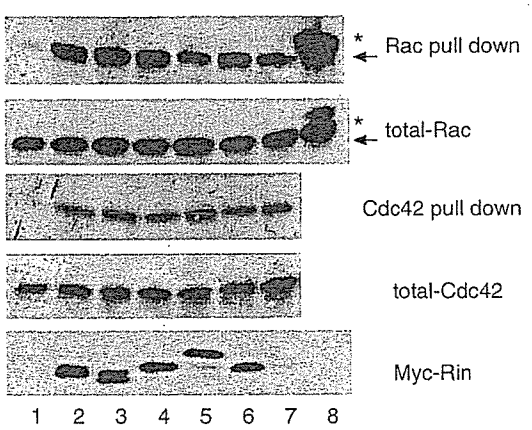

Figure 4. **Rin activates endogenous Rac/Cdc42 in PC12 cells.** Cells were transfected with an empty vector or Myc-tagged expression vectors encoding several Rin proteins. After 48 h, cells were lysed and cleared, followed by Rac/Cdc42 pull-down assay, as described in the Materials and methods. Bound endogenous Rac proteins (arrow) and Cdc42 proteins were visualized by Western blotting using an anti-Rac antibody and anti-Cdc42 antibody, respectively. Lane 1, empty vector; lane 2, wild-type Myc-Rin, lane 3, Myc-RinQ78L; lane 4, Myc-RinΔ18; lane 5, Myc-RinC-4; lane 6, Myc-RinC-7; lane 7, empty vector with 50 ng/ml NGF for 3 min; lane 8, constitutively active Myc-Rac (positive control, asterisk). Data are representative of three independent experiments, which gave essentially identical results.

CaM is also involved in Rin-mediated neurite outgrowth

Because Rin protein has the ability to interact with CaM directly (Lee et al., 1996), we conjectured that association of Rin with CaM might be required for Rin-mediated neurite outgrowth. To test this hypothesis, Rin-transfected PC12 cells were incubated with the CaM inhibitor W13. As shown in Fig. 5 (A and B), W13 could significantly inhibit the Rin-mediated neurite outgrowth. To exclude the possibility of nonspecific inhibitory effects of W13, we used W12, which is a structural analogue of W13 and is far less effective than W13 as a CaM inhibitor (Hidaka and Tanaka, 1983). The results showed that Rin-mediated neurite outgrowth was not affected by incubation with a concentration of W12 that was equivalent to the concentration of W13 that significantly inhibited the neurite outgrowth (Fig. 5, A and B). These data suggest that the CaM antagonist W13 has a specific inhibitory effect on the Rin-mediated neurite outgrowth.

A deletion mutant of Rin, RinΔ18, in which the COOH-terminal 18 residues of the CaM-binding motif were deleted (Fig. 5 C), could no longer bind to CaM (Fig. 5 D). This RinΔ18 mutant activated Rac/Cdc42 to a similar degree as the full length wild-type or constitutively active Rin protein (Fig. 4, lane 4). However, the RinΔ18 mutant failed to exhibit neurite outgrowth activity (Fig. 5, A and E).

To further confirm this observation, we constructed other CaM-binding defective mutants, which contained point rather than deletion mutation. These point mutants, named RinC-7 and RinC-4, in which all seven basic amino acid residues and four basic residues were replaced with neutral ones in the COOH-terminal of the Rin protein that was deleted in the RinΔ18 mutant, respectively (Fig. 5 C), also showed no binding activity to CaM (Fig. 5 D). As expected, they activated Rac/Cdc42 (Fig. 4, lanes 5 and 6), but failed to extend neurites in PC12 cells (Fig. 5, A and E). Together, these data strongly suggest that Rin-mediated neurite outgrowth requires both downstream Rac/Cdc42 activation and CaM association.

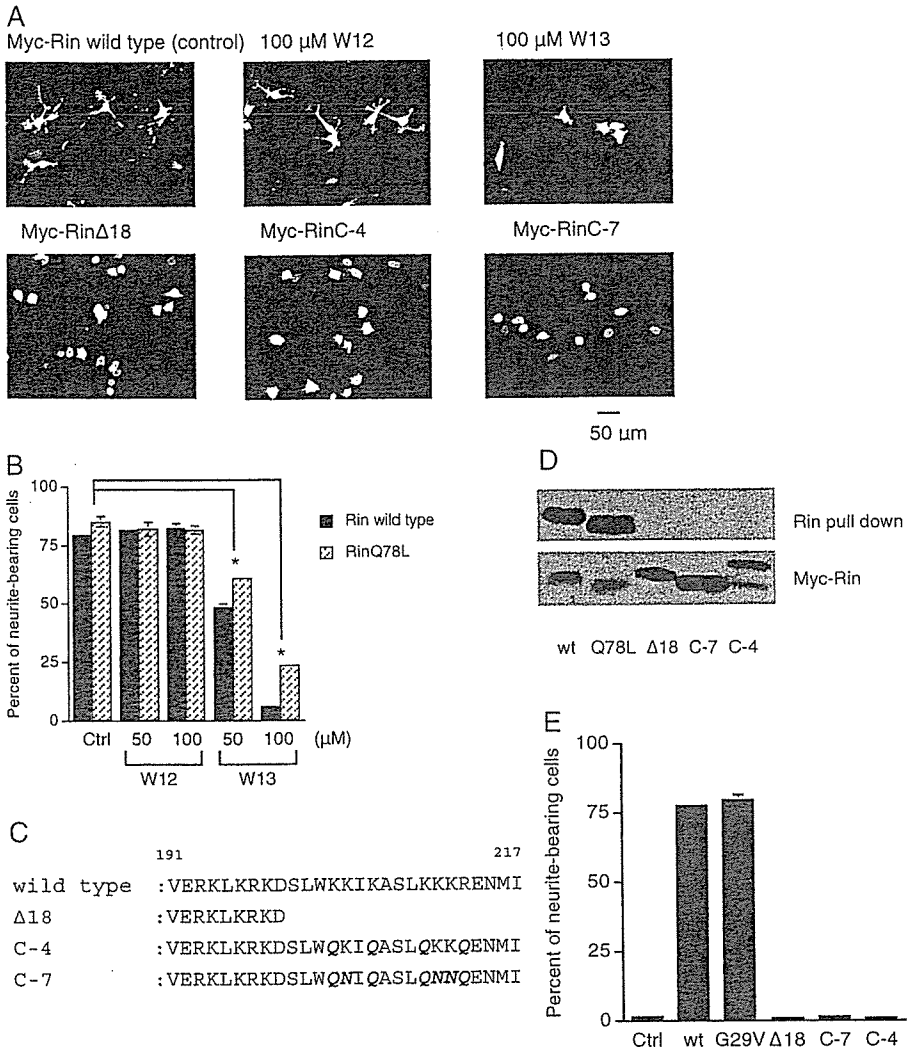

Figure 5. **CaM association is necessary for Rin-induced neurite outgrowth in PC12 cells.** (A, B) PC12 cells were transfected with Myc-tagged expression vectors encoding several Rin proteins and incubated with vehicle, 50 or 100 μM W13 (CaM antagonist) or W12 (inactive analogue of W13). After 48 h, cells were fixed and immunostained with an anti-Myc antibody. Columns and vertical bars denote the mean ± SEM, respectively ($n = 3$). Asterisks indicate $P < 0.05$. (C) Comparison of the COOH-terminal amino acid sequences (amino acids 191–217) of wild-type Rin protein, RinΔ18, RinC-4, and RinC-7. The residues of the mutant proteins that are different from those of the wild-type Rin protein are italicized. (D) Cos-7 cells were transfected with Myc-tagged expression vectors encoding several Rin proteins. After 48 h, cells were lysed, cleared, and Rin proteins were pulled down with CaM-conjugated agarose beads at 4°C for 2 h as described in the Materials and methods. Bound Myc-Rin protein was visualized with an anti-Myc antibody. Data are representative of three independent experiments, which gave essentially identical results. (E) PC12 cells were transfected with Myc-tagged expression vectors encoding several Rin mutant proteins. After 48 h, cells were fixed and immunostained with an anti-Myc antibody. Columns and vertical bars denote the mean ± SEM, respectively ($n = 3$).

Endogenous RhoA is activated in Rin-expressed cells

To examine whether Rho is also activated by Rin, we measured the endogenous Rho activity by Rho pull-down assay. This assay system makes use of the Rho-binding domain of mDia1 as a GST fusion protein, which specifically binds to and isolates the GTP-bound Rho (Kimura et al., 2000). As shown in Fig. 6 A, an increase of the amounts of GTP-bound Rho was detected in both the wild-type Rin-transfected (lane 2) and RinQ78L-transfected cell lysates (lane 3). The level of GTP-bound Rho was similar to the lysophosphatidic acid (LPA)-treated cells (Fig. 6 A, lane 7).

Next, we examined whether RhoA affects the morphology of Rin-expressed cells using RNA interference method. As shown in Fig. 6 B, short interfering RNA (siRNA) of RhoA eliminated the expression of RhoA protein, but did not eliminate the expression of another protein, such as Rac. Control siRNA did not eliminate the expression of RhoA protein (Fig. 6 B). These results indicate that siRNA of RhoA specifically disrupts RhoA protein expression. Disruption of RhoA function induced more branching points of Rin-induced neurites (Fig. 6 C, i.e., there were 2.84 ± 0.08 branching points per cell for RhoA-disrupting Rin-expressed cells, compared with 2.20 ± 0.08 branching points per cell for Rin-expressed cells; $P < 0.05$). siRNA of RhoA itself did not induce neurites in control PC12 cells (Fig. 6 C). RhoA is supposed to function as a negative regulator for neurites and dendrite branch formation (Li et al., 2000; Nakayama et al., 2000). Our data showed that Rin-induced neurite outgrowth was not simply due to RhoA inhibition, and that Rin may regulate the neurite complexity through activation of Rac/Cdc42 and RhoA.

Endogenous Rin protein is also involved in calcium-mediated neurite outgrowth

To investigate the function of the endogenous Rin protein, we examined whether expression of the dominant negative Rin protein altered the function of the endogenous Rin in PC12 cells. Rin mRNA was not detected in nonneuronal Cos-7 cells but certainly existed in PC12 cells, though its mRNA level is rather lower than that of primary culture of neuronal cells (Fig. 7 A). Next, we constructed the dominant negative Rin, RinS34N, in which Ser34 was replaced with Asn. The cognate S17N mutant of the Ras, which is regarded as a dominant negative Ras, cannot bind to the effectors but binds to its GEFs and sequesters them, with the result that it cannot activate its downstream signaling cascade (Vojtek and

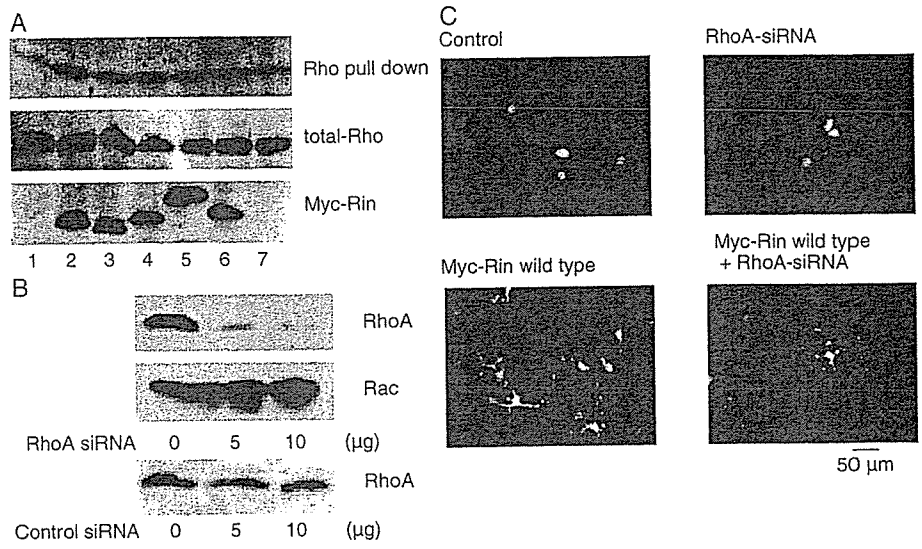

Figure 6. **Rin activates endogenous Rho in PC12 cells.** (A) PC12 cells were transfected with an empty vector or Myc-tagged Rin vector. After 48 h, cells were stimulated with vehicle or 10 μM LPA for 1 min. Cells were lysed and cleared, followed by Rho activation assay, as described in the Materials and methods. Lane 1, empty vector; lane 2, wild-type Myc-Rin, lane 3, Myc-RinQ78L; lane 4, Myc-RinΔ18; lane 5, Myc-RinC-4; lane 6, Myc-RinC-7; lane 7, empty vector with 10 μM LPA for 1 min. Data are representative of three independent experiments, which gave essentially identical results. (B) PC12 cells were transfected with indicated amounts of siRNA of RhoA or control siRNA. After 48 h, cells were lysed, cleared and followed by Western blotting as described in the Materials and methods. (C) PC12 cells were transfected with a Myc-tagged wild-type Rin vector and a siRNA of RhoA either alone or in pairs. After 48 h, cells were fixed and observed as described in the Materials and methods.

Der, 1998). However, RinS34N has quite a low expression efficiency compared with the wild-type protein (unpublished data). Therefore, we needed to construct another Rin mutant that act in a dominant negative manner. RinG29V-C-7, in which the CaM-binding motif of the constitutively active RinG29V protein was mutated in a manner similar to that for the RinC-7 mutant, was constructed. As shown in Fig. 7 B, Myc-tagged RinG29V-C-7 could not induce the neurite outgrowth in PC12 cells because of the lack of CaM-binding ability, and it also suppressed the wild-type Rin-mediated neurite outgrowth. These data suggest that RinG29V-C-7 can act as a dominant negative Rin.

PC12 cells expressed RinG29V-C-7 proteins inhibit neither the NGF-induced neurite outgrowth (Fig. 7 C), nor the NGF-induced Rac/Cdc42 activation (Fig. 7 D). These data indicate that Rin is not likely to be involved in the NGF-mediated signaling pathway leading to neurite outgrowth.

It was reported previously that elevation of extracellular potassium evokes membrane depolarization, and that depolarization-induced calcium entry through voltage-dependent calcium channels sustains neurites and cell survival after NGF withdrawal in PC12 cells (Teng and Greene, 1993). Moreover, Mark et al. (1995) have reported that intracellular cAMP and KCl depolarization synergistically stimulate neurite outgrowth in PC12 cells. Therefore, we investigated whether Rin is involved in calcium entry-mediated neurite outgrowth after KCl-evoked membrane depolarization in PC12 cells.

As shown in Fig. 7 E, ~30% of 50 μM forskolin-treated GFP-expressed cells showed neurite outgrowth. After addition of 50 mM KCl, neurite outgrowth of forskolin-stimulated cells was potentiated by KCl-evoked membrane-depolarization and subsequent calcium entry (Fig. 7 E). As demonstrated previously (Mark et al., 1995), depolarization by KCl alone showed no significant induction of neurite outgrowth (not depicted), and forskolin and KCl depolarization-induced neurite outgrowth was calcium entry-dependent because it was inhibited by the L-type calcium channel blockers nitrendipine and diltiazem (Fig. 7 E). Dominant negative RinG29V-C-7 could not inhibit the forskolin-induced neurite outgrowth, but could inhibit the neurite outgrowth stimulated by forskolin and KCl at the level of the stimulation of forskolin alone (Fig. 7 E). After preincubation with the L-type calcium channel blockers nitrendipine or diltiazem, RinG29V-C-7 was unable to further inhibit the neurite outgrowth stimulated by forskolin and KCl, as compared with the forskolin and KCl-stimulated blocker-pretreated cells (Fig. 7 E).

To confirm these findings, we examined whether Rin is certainly involved in the calcium entry-mediated neurite outgrowth by using RNA interference method. As shown in Fig. 7 F, siRNA of Rin eliminated the expression of Rin protein, but did not eliminate the expression of another protein, such as Ras. Control siRNA did not eliminate the expression of Rin protein (Fig. 7 F). These results indicate that siRNA of Rin specifically disrupts Rin protein expression. The neurite outgrowth stimulated by forskolin and KCl is inhibited at the level of the stimulation of forskolin alone after siRNA of Rin introduction (Fig. 7 G). Control siRNA did not show this inhibitory phenomenon (Fig. 7 G). These data suggested that dominant negative Rin or siRNA of Rin inhibit calcium-mediated neurite outgrowth and that Rin may be involved in the calcium-mediated signaling pathways leading to neurite outgrowth.

In addition, we examined the effect of inhibiting Rac/Cdc42 in this calcium-mediated neurite outgrowth. As shown in Fig. 7 H, dominant negative Rac or Cdc42 considerably inhibited neurite outgrowth after forskolin stimulation. Dominant negative Cdc42-expressed cells showed the potentiation of neurite outgrowth after KCl addition, and siRNA of Rin did not inhibit this potentiation further (Fig. 7 H). These data suggest that Rin requires Cdc42 signaling

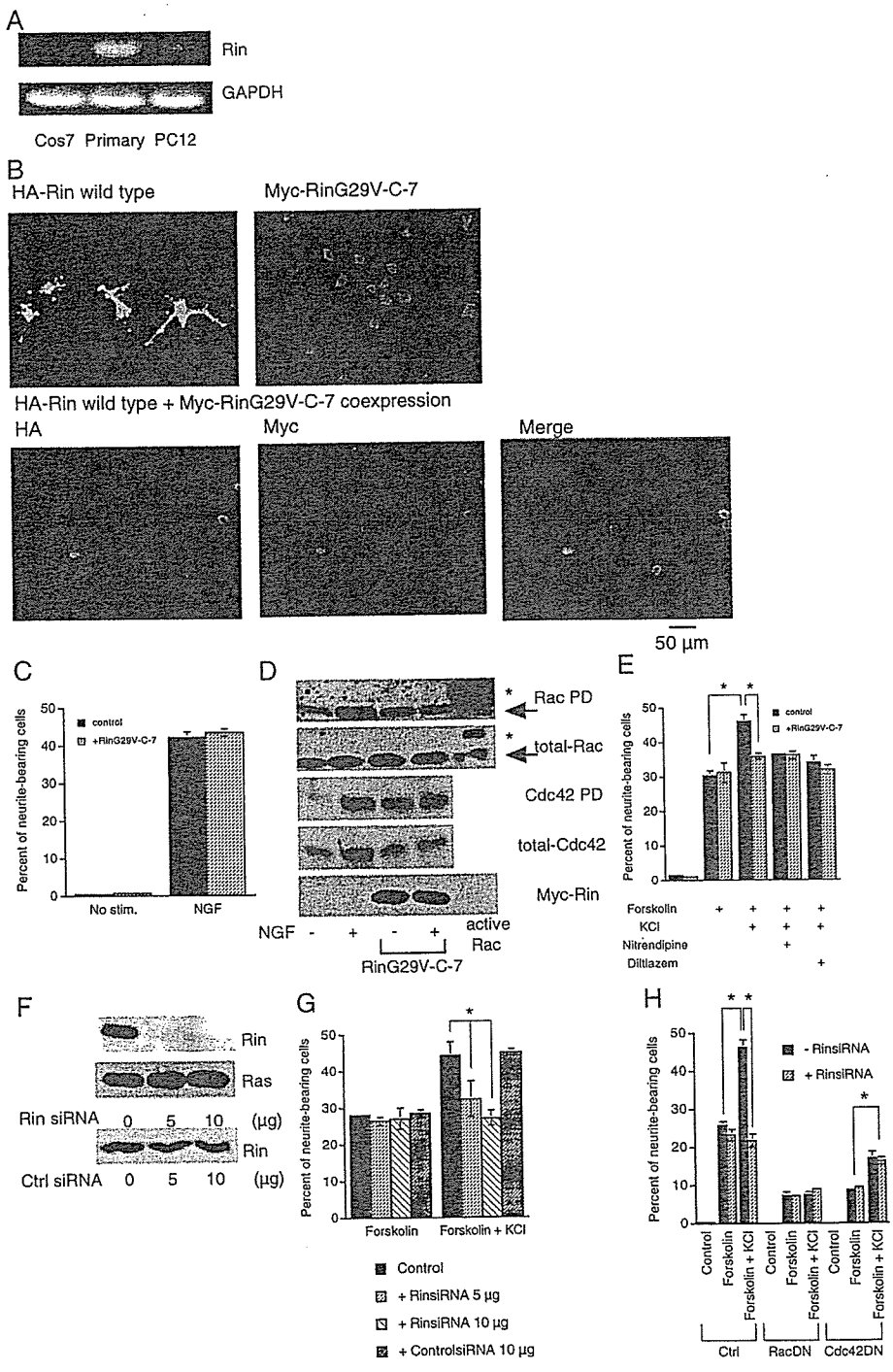

Figure 7. **Endogenous Rin protein is involved in calcium-mediated neurite outgrowth in PC12 cells.** (A) The expression of Rin and GAPDH (constitutively expressed gene) at the mRNA level was detected by performing RT-PCR from total RNA isolated from Cos-7, PC12, and primary dissociated neuronal cells from P3 mouse brain, as described in the Materials and methods. (B) PC12 cells were transfected with an HA-tagged wild-type Rin vector and a Myc-tagged vector encoding RinG29V-C-7 mutant protein either alone or in pairs. After 48 h, cells were fixed and immunostained with an anti-HA antibody and an anti-Myc antibody. In the merge, HA-Rin staining is shown in green (using FITC-labeled anti–rat secondary antibody), whereas Myc-Rin staining is shown in red (using Cy3-labeled anti–mouse secondary antibody). (C) PC12 cells were transfected with an empty vector or a Myc-tagged RinG29V-C-7 expression vector. After 4 h, transfected cells were stimulated with vehicle or 50 ng/ml NGF for 44 h. Cells were fixed and immunostained with an anti-Myc antibody. Columns and vertical bars denote the mean ± SEM, respectively ($n = 3$). (D) PC12 cells were transfected with an empty vector or RinG29V-C-7 expression vector. After 48 h, they were stimulated with vehicle or 50 ng/ml NGF for 5 min. Cells were lysed and cleared, followed by a Rac/Cdc42 pull-down assay (Rac PD and Cdc42 PD). Bound endogenous Rac proteins (arrow) and Cdc42 proteins were visualized by Western blotting. Constitutively active Myc-Rac (positive control) is indicated by asterisk. Data are representative of three independent experiments, which gave essentially identical results. (E) PC12 cells were transfected with an empty vector or a Myc-tagged RinG29V-C-7 expression vector. After 4 h, transfected cells were pretreated with vehicle or the L-type calcium channel blocker nitrendipine (final 10 μM)/diltiazem (final 50 μM) for 30 min and stimulated with 50 μM forskolin alone or 50 μM forskolin plus 50 mM KCl for 44 h. Cells were fixed and immunostained with an anti-Myc antibody. Columns and vertical bars denote the mean ± SEM, respectively ($n = 3$). Asterisks indicate $P < 0.05$. (F) PC12 cells were transfected with 1 μg of Myc-tagged wild-type Rin vector and indicated amounts of siRNA. After 48 h, cells were lysed, cleared and followed by Western blotting as described in the Materials and methods. (G) PC12 cells were transfected with 1 μg of pGFP-C1 vector and indicated amounts of siRNA. After 4 h, transfected cells were stimulated with 50 μM forskolin alone or 50 μM forskolin plus 50 mM KCl for 44 h. Cells were fixed and counted as described in the Materials and methods. Columns and vertical bars denote the mean ± SEM, respectively ($n = 3$). The asterisk indicates $P < 0.05$. (H) PC12 cells were transfected with 1 μg of Myc-tagged RacS17N/Cdc42S17N and 1 μg of pGFP-C1 vector plus 10 μg of Rin-specific siRNA either alone or in pairs. After 4 h, transfected cells were stimulated with 50 μM forskolin alone or 50 μM forskolin plus 50 mM KCl for 44 h. Cells were fixed and counted as described in the Materials and methods. Columns and vertical bars denote the mean ± SEM, respectively ($n = 3$). Asterisks indicate $P < 0.05$.

pathway to mediate calcium-induced neurite outgrowth. However, dominant negative Rac-expressed cells did not show the potentiation after KCl addition (Fig. 7 H). Thus, it is uncertain whether Rac is specifically required for Rin-mediated calcium-induced neurite outgrowth.

Discussion

Here, we presented evidence that Rin protein plays an important role in neuronal calcium signaling. We found that Rin protein did not activate MAPK and that MAPK inhibi-

tion did not suppress Rin-induced neurite outgrowth. Previous reports also indicated that Rin fails to activate MAPK, Jun NH_2-terminal kinase or p38 kinase (Rusyn et al., 2000; Spencer et al., 2002). Kobayashi et al. (1997) showed previously that constitutively active PI3K can induce Jun NH_2-terminal kinase and lead to neurite outgrowth in PC12 cells. Because GTP-bound Ras interacts with the p110 catalytic subunit of PI3K (Bos, 1998; Vojtek and Der, 1998; Reuther and Der, 2000), we examined whether Rin is able to interact with PI3K using the coimmunoprecipitation method. Although Rin and Ras share high sequence identity within the effector domains (Lee et al., 1996), we could not detect Rin interaction with the PI3K p110 subunit (unpublished data), as reported previously (Shao et al., 1999). Thus, Rin is likely to use neither the MAPK cascade nor the PI3K cascade that lead to neurite outgrowth in PC12 cells.

We found that wild-type Rin, as well as constitutively active RinQ78L, induced neurite outgrowth. We (Hoshino and Nakamura, 2002) and Spencer et al. (2002) observed previously that basal levels of GTP-bound wild-type Rin remains quite high and that the amount of wild-type Rin precipitated from the Cos-7 cell lysates is almost the same as that of constitutively active Rin using a Rin pull-down assay system (unpublished data). Considering that the guanine nucleotide dissociation rate of Rin is faster than that of most Ras family member (Shao et al., 1999) and that the intracellular concentration of GTP is much higher than that of GDP (McCormick, 1989), it is expected that most of Rin proteins may be remained active GTP-bound state in the cells. There may be another possibility that it might be based on low activity of RinGAP or that a specific GEF of Rin might be exist and might exhibit marked affinity and catalytic efficiency for wild-type Rin protein.

Spencer et al. (2002) reported previously that neither GFP-tagged wild-type Rin nor GFP-tagged RinQ78L induces neurite outgrowth in PC6 cells, which is a subline of PC12 cells. This discrepancy may be due to the difference of the cell lines. The large size of GFP (27 K) could interfere with the distribution and function of the fusion protein. In fact, we verified that neither GFP-tagged wild-type Rin nor GFP-tagged RinQ78L induced neurite outgrowth in PC12 cells (unpublished data). To circumvent this problem, we transfected tiny tag-fused (Myc-tagged or HA-tagged) Rin into the pEF-Bos vector, which is a powerful mammalian expression vector (Mizushima and Nagata, 1990).

We demonstrate that Rac/Cdc42 activity is required for the Rin-induced neurite outgrowth and that Rin activates endogenous Rac/Cdc42 in PC12 cells. To confirm this observation, we cotransfected cells with wild-type Rin and dominant negative PAK1 protein, one of the effector molecules of Rac/Cdc42 proteins (Zhao et al., 1998). Dominant negative PAK1 protein also suppressed the Rin-mediated neurite outgrowth. (There were 76.45 $\pm$ 2.00% of neurite-bearing cells for wild-type Rin-expressed cells, compared with 59.82 $\pm$ 1.14 of neurite-bearing cells for dominant negative PAK1 and wild-type Rin-coexpressed cells; $P < 0.05$). To examine whether Rin directly associates with Rac/Cdc42, we performed the coimmunoprecipitation assay. As a result, we failed to detect the direct interaction between Rin and Rac/Cdc42 (unpublished data). Probably, there must be a linking molecule between Rin and Rac/Cdc42, or their GEFs, such as Vav or Cdc24. Because RhoG is shown to be located upstream of Rac/Cdc42 (Kato et al., 2000), we investigated whether RhoG participated in the Rin and Rac/Cdc42 pathway using RNA interference method. As a result, RhoG is not likely to be involved in Rin-mediated neurite outgrowth (unpublished data). Identification of a molecular link between Rin and Rac/Cdc42 should be further clarified.

We showed that CaM association with Rin is necessary to induce neurite outgrowth. We did not analyze the downstream target of CaM, but there is a possibility that calcium/CaM-dependent protein kinases (CaMKs) and/or IQGAP1 are the targets. CaMKI and CaMKII are enriched in neuronal processes and synapses (Curtis and Finkbeiner, 1999), and they can phosphorylate the serine 133 of cAMP response element binding protein, a well-known transcription factor involved in synaptic plasticity (Curtis and Finkbeiner, 1999). IQGAP1 has an affinity for CaM through its IQ motif and an actin-binding protein, whose function is cross-linking the actin filaments into bundles (Hart et al., 1996). IQGAP1 is also a Rac/Cdc42 effector and serves as a direct molecular link between Rac/Cdc42 and actin filaments under the regulation of CaM (Hart et al., 1996; Bashour et al., 1997). Recently, Rac/Cdc42 has been shown to interact with microtubules through IQGAP1 and CLIP-170, a microtubule plus end tracking protein, and forms a complex at the leading edge, resulting in a polarized microtubule array and cell polarization (Fukata et al., 2002). We examined whether IQGAP1 associates Rin–CaM complex and found that IQGAP1 formed a ternary complex with Rin and CaM by coimmunoprecipitation assay (unpublished data). There is a possibility that CaMK and/or IQGAP1 might contribute to the Rin-mediated neurite outgrowth.

We found that Rho is also activated by Rin. Rho family proteins are central regulators of neuronal morphology including neurite branching (Luo, 2000). We found that Rin-induced neurite has a plenty of branchings. It has been shown that Rac/Cdc42 are positive regulators for dendritic branching and remodeling whereas Rho is a negative regulator for branch formation (Li et al., 2000; Nakayama et al., 2000). It is an interesting possibility that Rin may induce the branchings of neurite by exquisite balancing between the downstream Rac/Cdc42 and Rho signaling.

We investigated the function of endogenous Rin using dominant negative Rin. In RT-PCR analysis, the expression of Rin at the mRNA level in PC12 cells was low. For this reason, the endogenous Rin expression in PC12 cells was too low to detect with Western blotting using an anti-Rin antibody (unpublished data). At first, we constructed a RinS34N expression vector, but it could not be efficiently expressed in the cells, probably due to the cell toxicity of RinS34N. This fact indicates that endogenous Rin may play an important role in regulating the cell growth. Then, we made another dominant negative Rin mutant vector encoding RinG29V-C-7, which can be efficiently expressed in the cells. It was expected that RinG29V-C-7 can bind the effector molecules through their effector region but suppress signals to the downstream molecules leading to the neurite outgrowth. We have shown that dominant negative RinG29V-C-7 could not inhibit the NGF-induced neurite outgrowth. Spencer et al. (2002) demonstrated previously that domi-